Strong Pion–Alpha-Particle Scattering with Electromagnetic Corrections*

RONALD A. CHRISTENSEN
Lawrence Radiation Laboratory, University of California, Berkeley, California 94720
(Received 11 June 1969)

Electromagnetic corrections to $\pi\alpha$ scattering for spacelike q^2 are calculated to see whether they can be used to determine r_π. The low-momentum t dependence of the off-shell strong amplitude used in this calculation is determined with the help of crossing symmetry, current algebra, and the hypothesis of partially conserved axial-vector current. The relativistic corrections are found to be just as important as those which are also included in nonrelativistic treatments. When only the nonrelativistic terms are used, the large value of r_π (2–3 F) obtained recently from $\pi^\pm\alpha$ scattering is reproduced. Including the relativistic terms brings the resulting value of r_π down to approximately 1 F. This is consistent with the values obtained by using inelastic electron-proton scattering; however, the $\pi^\pm\alpha$ results are quite sensitive to the details of the $\pi\alpha$ nuclear interaction and to the relativistic effects, which are only roughly approximated.

I. INTRODUCTION

A FEW years ago Sternheim and Hofstadter[1] proposed that the electromagnetic structure of the pion be studied by considering the scattering of $\pi^\pm$ on zero-isospin nuclei such as ^{4}He. (Table I shows determinations of the pion charge radius based on other techniques.) A formalism was developed by Schiff[2] for calculating the nonrelativistic Coulomb effects of elastic $\pi^\pm\alpha$ scattering to first order in the fine-structure constant without the use of Coulomb wave functions. (See Appendix A for a review of Schiff's formalism and methods of adapting it to experimental data.) It was demonstrated that even in nonrelativistic theory first-order Coulomb effects arise not only from the Born

TABLE I. Predicted and measured values of r_π.

Source	r_π (F)	Comments
		Theoretical
Nambu,[a] Sakurai,[b] Gell-Mann and Zachariasen,[c] and Gell-Mann[d]	0.6	Vector-dominance model
Salecker[e]	0.82	Disperson relation and $J=T=1$ $\pi\pi$ effective-range expansion
Cocho and Ar-Rashid[f]	0.4	Current algebra excluding A_1 meson
Cocho and Ar-Rashid[f]	1.4	Current algebra including A_1 meson
Efremov[g]	0.3	Approx. to equation based on minimal electromagnetic coupling
Barut[h]	1.7	Electromagnetic current in $O(4,2)$
Arnowitt *et al.*[i]	0.6	$SU(2)\otimes SU(2)$ current algebra and meson dominance
Roos and Pisut[j]	0.628±0.004	Analysis of $e^+ + e^- \to \pi^+ + \pi^-$
Roos and Pisut[j]	0.7	Analysis of $e^- + p \to e^- + n + \pi^+$
Shrauner *et al.*[k]	0.36±0.12	Self-consistent multiple-quark πp scattering analysis
Oyanagi[l]	0.83	Veneziano-type formula
		Experimental
Allen *et al.*[m]	<4.5	$\pi^- + e^- \to \pi^- + e^-$, $q^2=0.00004$ to 0.004 $(\mathrm{GeV}/c)^2$
Cassel[n]	<3.3	$\pi^- + e^- \to \pi^- + e^-$, $q^2=0.003$ to 0.01 $(\mathrm{GeV}/c)^2$
Akerlof *et al.*[o]	0.8±0.1	$e^- + p \to e^- + n + \pi^+$, $q^2=0.05$ to 0.4 $(\mathrm{GeV}/c)^2$
Mistretta *et al.*[p]	0.86±0.14	$e^- + p \to e^- + n + \pi^+$, $q^2=0.04$ to 0.2 $(\mathrm{GeV}/c)^2$
Auslander *et al.*[q]	0.632±0.009	$e^+ + e^- \to \pi^+ + \pi^-$, $q^2=-0.4$ to -0.8 $(\mathrm{GeV}/c)^2$
Augustin *et al.*[r]	0.628±0.003	$e^+ + e^- \to \pi^+ + \pi^-$, $q^2=-0.4$ to -0.7 $(\mathrm{GeV}/c)^2$
Devons *et al.*[s]	<1.9	$\pi^- + p \to n + e^+ + e^-$, $q^2=-0.002$ to -0.02 $(\mathrm{GeV}/c)^2$

[a] Y. Nambu, Phys. Rev. **106**, 1366 (1957).
[b] J. J. Sakurai, Ann. Physik **11**, 1 (1960).
[c] M. Gell-Mann and F. Zachariasen, Phys. Rev. **124**, 953 (1961).
[d] M. Gell-Mann, Phys. Rev. **125**, 1067 (1962).
[e] H. Salecker, Z. Physik **164**, 463 (1961).
[f] G. Cocho and H. Ar-Rashid, Progr. Theoret. Phys. (Kyoto) **36**, 1150 (1966).
[g] A. V. Efremov, Zh. Eksperim. i Teor. Fiz. **53**, 732 (1968) [English transl.: Soviet Phys.—JETP **26**, 455 (1968)].
[h] A. O. Barut, Nucl. Phys. **B4**, 455 (1968).
[i] R. Arnowitt *et al.*, Phys. Rev. **174**, 2008 (1968).
[j] M. Roos and J. Pisut, Nucl. Phys. **B10**, 563 (1969).
[k] E. Shrauner *et al.*, Phys. Rev. **181**, 1930 (1969).
[l] Y. Oyanagi, Report No. UT-16 1969 (unpublished).
[m] J. Allen *et al.*, Nuovo Cimento **32**, 1144 (1964).
[n] D. G. Cassel, thesis, Princeton University, 1965 (unpublished).
[o] C. W. Akerlof *et al.*, Phys. Rev. **163**, 1482 (1967).
[p] C. Mistretta *et al.*, Phys. Rev. Letters **20**, 1523 (1968).
[q] V. L. Auslander *et al.*, Phys. Letters **25B**, 433 (1967).
[r] J. E. Augustin *et al.*, Phys. Rev. Letters **20**, 126 (1968); Phys. Letters **28B**, 508 (1969).
[s] S. Devons, P. Nemethy, and S. Nissim-Sabat, Report No. INFN-ROME-202, 1968 (unpublished).

* Work supported by the U. S. Atomic Energy Commission.
[1] M. M. Sternheim and R. Hofstadter, Nuovo Cimento **38**, 1854 (1965).
[2] L. I. Schiff, Progr. Theoret. Phys. (Kyoto) Suppl. Extra Number, 400 (1965); Progr. Theoret. Phys. (Kyoto) **37**, 635 (1967).

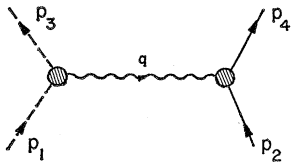

FIG. 1. First-order Coulomb Born amplitude, $A_{C,B}$.

amplitude (Fig. 1), but also from distortion of the pion wave function by the nuclear interaction. The nonrelativistic distortion terms arise when the pion, in the process of a Born Coulomb interaction with the α particle, also experiences a nuclear interaction, as shown in Figs. 2(e) and 2(f). [Since the nonrelativistic Coulomb potential acts instantaneously, it does not include the purely relativistic diagrams shown in Figs. 2(a)–2(d), 2(g)–2(n), and 3.]

Three $\pi^{\pm}\alpha$ scattering experiments have been performed at Rochester,[3] Northwestern,[4] and Berkeley,[5] and there are at least three different methods of adapting Schiff's formalism to the data due to West,[6,7] Block,[8] and Auerbach *et al.*[9] The results, given in Refs. 3–9, of applying these methods of analysis to these sets of data are listed in Table II.[10,11]

If we keep in mind the prediction $r_\pi \approx 0.63$ F of the vector-dominance model,[12] we find several disconcerting features concerning these results. The first experiment, at Rochester, contained only eight data points, and fits to these data are not good statistically, principally because of one apparently anomalous point. However, if this point is omitted, the upper limit on r_π is much larger than 1.5 F.

The second set of data, from Northwestern, contains such large experimental errors that it is difficult to see

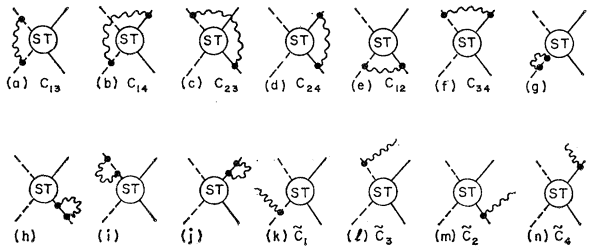

FIG. 2. First-order external terminating corrections. The diagrams in which one or two legs of the strong interaction are off shell contribute to the off-shell correction terms C_{ij} or $\tilde{C}_i$ as indicated. The on-shell term B_{13} comes from (a), (g), and (i), and $\tilde{B}_{13}$ comes from (k) and (l), and similary for the other B_{ij}'s and $\tilde{B}_{ij}$'s.

any $F_\pi(q^2)$ effect in all the noise. In fact, some best fits to this data are obtained for negative values of r_π^2.

Finally, the most complete (60 points) and most accurate ($\approx 3\%$ errors in $d\sigma^{(\pm)}/d\Omega$) experiment, at Berkeley, using the method of analysis which fits the data best, yields astonishingly large values for r_π.

In order to determine whether or not these results indicate that the vector-dominance model (which appears to be valid near $q^2 \approx -m_\rho^2$) fails to extend to spacelike q^2, it is necessary to reexamine the effect of $F_\pi(q^2)$ upon $\pi^{\pm}\alpha$ elastic scattering.

The basic problem involved in extracting $\pi\pi\gamma$ vertex information from $\pi^{\pm}\alpha$ scattering data is that of calculating the distortion amplitude corresponding to all diagrams involving both strong and Coulomb interactions. Two questions concerning this calculation have received inadequate attention. The first problem concerns the validity of applying a nonrelativistic calculation to data involving momentum transfers in the order of the pion mass. (The value of q^2 in the three experiments ranged from $0.34m_\pi^2$ to $1.22m_\pi^2$.) The relativistically complete set of first-order distortion diagrams is given in Figs. 2 and 3.[13] The nonrelativistic calculation uses only the low-momentum limits of Figs. 2(e) and 2(f).

The corrections in which the photon terminates on external lines, those shown in Fig. 2, can be computed

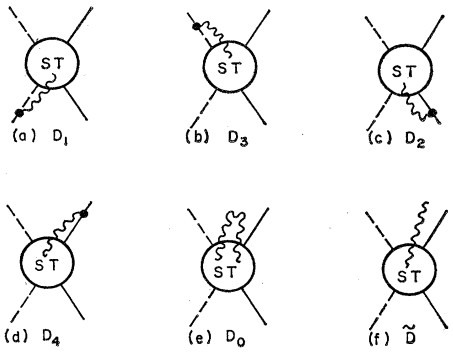

FIG. 3. First-order internal terminating corrections.

[3] M. E. Nordberg and K. F. Kinsey, Phys. Letters **20**, 692 (1966).
[4] M. M. Block *et al.*, Phys. Rev. **169**, 1074 (1968).
[5] K. M. Crowe, A. Fainberg, J. Miller, and A. S. L. Parsons, Phys. Rev. **180**, 1349 (1969). See also A. Fainberg, UCRL Report No. UCRL-19208, 1969 (unpublished).
[6] G. B. West, J. Math. Phys. **8**, 942 (1967).
[7] G. B. West, Phys. Rev. **162**, 1677 (1967).
[8] M. M. Block, Phys. Letters **25B**, 604 (1967).
[9] E. H. Auerbach, D. M. Fleming, and M. M. Sternheim, Phys. Rev. **162**, 1683 (1967).
[10] Ingoring distortion entirely, the Rochester data give $r_\pi = 1.8 \pm 0.8$ F.
[11] If the Kisslinger model rather than a Gaussian potential is used, a better fit is obtained, giving $r_\pi = 2.26 \pm 0.16$ F.
[12] The vector-dominance model gives (ignoring Γ_ρ) $F_\pi(q^2) = 1/(1+q^2/m_\rho^2)$, which implies a mean pion charge radius of $r_\pi = (\sqrt{6})/m_\rho = 0.63$ F; see M. Gell-Mann, Phys. Rev. **125**, 1067 (1962). The storage ring $e^+e^- \to \pi^+\pi^-$ measurements at timelike momentum transfers $[-0.7 \lesssim q^2 \lesssim -0.4$ (BeV/c)^2] fit this form fairly well, but suggest $r_\pi \approx 0.8$ F: J. E. Augustin *et al.*, Phys. Rev. Letters **20**, 126 (1968); V. L. Auslander *et al.*, Phys. Letters **25B**, 433 (1967). The inelastic electron-proton scattering $e^-p \to e^-n\pi^+$ measurements at spacelike momentum transfers $[0 < q^2 \leq 0.5$ (GeV/c)^2], after considerable interpretation, seem to suggest $r_\pi \approx 0.86 \pm 0.14$ F: C. W. Akerlof *et al.*, Phys. Rev. **163**, 1482 (1967); C. Mistretta *et al.*, Phys. Rev. Letters **20**, 1523 (1968). The electron-pion scattering measurements at spacelike q^2 are easier to interpret but less accurate, giving only $r_\pi \leq 3$ F: J. Allen *et al.*, Nuovo Cimento **32**, 1144 (1964).
[13] We treat the α particle as an elementary particle, defining elastic scattering as leaving the α unexcited.

TABLE II. Pion charge raidus r_π (in F) based on nonrelativistic $\pi^{\pm}\alpha$ scattering analyses. Indicated error ranges are 1 s.d. (standard deviation) unless otherwise specified.

Experiment	q^2 [(GeV/c)^2]	Method of analysis West	Block	Auerbach
			$\leq$0.1 (1 s.d.)	$\leq$1.0 (1. s.d.)
Rochester[a]	0.005–0.03	$\leq$1.5	$\leq$0.9 (2 s.d.)	$\leq$2.0 (2 s.d.)
Northwestern	0.005–0.08		$\leq$0.9 (1 s.d.)	
			$\leq$2.1 (2 s.d.)	
Berkeley	0.005–0.09	$\leq$1.20 (1 s.d.)	1.29$\pm$0.82	2.88$\pm$0.37
		$\leq$1.77 (2 s.d.)	b	

[a] Reference 10.
[b] Reference 11.

by standard techniques once the off-shell $\pi^0\alpha$ strong-interaction elastic amplitude, which we denote by A_{ST}, is known. [These calculations are simplified by treating the external α legs as so massive that, with maximum momentum transfer in the order of m_π, they remain essentially on shell,[14] i.e., $A(p\pm q)\approx A(p)$, where p is the on-shell α momentum, over the range of photon momentum q giving the dominant contribution to the distortion.] We find that Figs. 2(b) and 2(c) are just as important as Figs. 2(e) and 2(f), while the rest of the external terminating corrections are negligible.

A complete computation of the corrections in which the photon terminates on internal lines (Fig. 3) requires knowledge of the off-shell amplitude A_μ for $\pi\alpha\rightarrow\pi\alpha\gamma$ (at least up to a scalar constraint). Given A_{ST}, using Ward's identity, and noting the absence of infrared divergences for internal terminating diagrams, we are able to determine A_μ up to terms of order q in the photon momentum. This is sufficient to enable us to show that Fig. 3(f) is negligible for the momentum transfers and resolutions involved in the experiments of interest. However, we need A_μ up to a scalar constraint to know the hard-photon contributions to the $p^\mu A_\mu$ parts of Figs. 3(a)–3(e). It appears that without strong-interaction information beyond the $\pi^0\alpha$ elastic amplitude, computation of these contributions must involve additional unknown parameters. To avoid this problem we assumed soft-photon dominance of the integral over $p^\mu A_\mu$ [see Eq. (49) below].

It turns out that the purely relativistic contributions add to the distortion effect obtained using only the nonrelativistic terms. (Ignoring hard internal terminating photons, this result is independent of the model and of the over-all phase of the amplitude, and arises purely from the relative phase conventions of Feynman diagrams.) Qualitatively, this provides the pion with more ways of interacting electromagnetically with the α particle, thereby making it possible to reproduce the observed electromagnetic distortion of the strong interaction using a smaller pion charge radius. With only nonrelativistic terms, on the other hand, a larger pion charge radius must be used to explain the magnitude of the distortion.

The second problem concerns the sensitivity of the value of r_π extracted from the data to the detailed structure of the strong interaction. The philosophy of the calculation is that the cross-section average data are used to fix A_{ST} and this is used together with cross-section difference data to determine r_π. However, the constraint that the form used for the strong amplitude A_{ST} fit the average data leaves certain leeway in A_{ST} which can affect r_π. There are features of A_{ST} to which r_π is sensitive, but the average cross section is not. The over-all phase of A_{ST} is an example, and is easily handled by simply including it as a parameter in the r_π determination (cross-checking this against what total cross-section data there are via the optical theorem). But there are more serious difficulties. Higher partial waves ($l=3$ and higher) could possibly affect the phase of A_{ST}, thereby influencing r_π, and yet not be seen in the average data. Also, the off-shell behavior of A_{ST}, which can only be crudely estimated from the average data, can affect r_π.

Except for the unlikely possibility of higher partial waves contributing *only* to the phase of A_{ST}, there appears to be no evidence for the presence of $l=3$ or higher waves of sufficient amplitude to influence r_π significantly. Also, if the on-shell behavior of the off-shell amplitude used is taken as indicitative of the accuracy of the amplitude off the mass shell, then the resulting error in r_π is small. However, there is presently no way of estimating the actual error off the mass shell. If the off-shell behavior is significantly more in error than the on-shell behavior, the resulting uncertainty in r_π can be quite large.

II. FIRST-ORDER ELECTROMAGNETIC EFFECTS

A. General Considerations

The order-α^1 corrections to any strong-interaction process can be grouped into three categories. First there are the Coulomb Born terms in which photons link otherwise disjoint parts. The first-order Coulomb Born term for elastic $\pi^{\pm}\alpha$ scattering occurs only in the

[14] More precisely, we keep α legs external to the strong interaction on shell everywhere in our formulation except in propagator terms $[(p_{2,4}\pm q)^2-m_\alpha{}^2]^{-1}$.

t channel (Fig. 1),

$$A_{C,B}=-\tfrac{1}{2}z_\pi[(s-u)/t]F_\pi(q^2)F_\alpha(q^2), \quad (1)$$

where $q=\sqrt{(-t)}=2k\sin\frac{1}{2}\theta$, $z_\pi=\pm1$ for $\pi^\pm$, the α-particle form factor[15] is $F_\alpha(q^2)=\exp(-\frac{1}{6}r_\alpha{}^2q^2)$, and we write the pion form factor[16] as $F_\pi(q^2)=1/(1+\frac{1}{6}r_\pi{}^2q^2)$.

Second, there are those corrections in which the extra photon line terminates only on hadrons external to the strong interaction (Fig. 2). In some of these [Figs. 2(a)–2(j)] the extra photon is virtual, whereas in others [Figs. 2(k)–2(n)] it is a real infrared photon. Both the real and the virtual photon terms can be split into a part which depends only on the on-shell strong amplitude and a part which depends on its off-shell behavior. The on-shell parts of the real and virtual photon contributions have compensating infrared divergences.[17] The finite residue of these on-shell parts contributes, in first order, a factor $1+2\alpha(\tilde{B}+\mathrm{Re}B)$ to the strong scattering cross section, where the real photon contribution $\tilde{B}$ and the virtual photon contribution B are given by Yennie, Frautschi, and Suura.[18] The real and virtual off-shell parts, which we will call $\tilde{C}$ and C, cannot in general be expressed as a simple multiplicative contribution to the strong scattering, since their structure is dependent upon the details of the strong-interaction model used.

Finally, there are the terms, which we will call $\tilde{D}$ and D, corresponding to diagrams in which at least one end of the extra photon (real or virtual) terminates on a line internal to the strong interaction (see Fig. 3). These terms also have a model-dependent structure.

All these first-order corrections considered, the $\pi^\pm\alpha$ elastic scattering cross section is

$$\frac{d\sigma^{(\pm)}}{d\Omega}=\frac{4}{s}\Big\{|A_{ST}|^2[1+2\alpha(\tilde{B}+\mathrm{Re}B)]+2\alpha\,\mathrm{Re}A_{ST}{}^*(A_{C,B}+C+D)+\alpha\sum_{\pm}\int^{\omega_q<\Delta E}\frac{d^3q}{(2\pi)^3 2\omega_q}|\tilde{C}+\tilde{D}|^2\Big\}, \quad (2)$$

where A_{ST} is the strong scattering amplitude and ΔE is the mimimum detectable photon energy in the particular experiment.

We next separate the terms which contribute to the cross-section difference $d\sigma^{(+)}-d\sigma^{(-)}$, where $(\pm)$ is the pion charge, from those which contribute to the average. To do this we let i, j be hadron leg indices (taking $i=1, 2, 3, 4$ as labeled in Fig. 1, and letting $i=0$ represent any internal line), specifying where the photon terminates:

$$B=\sum_{i<j}B_{ij}, \quad (3a)$$

$$\tilde{B}=\sum_{i<j}\tilde{B}_{ij}, \quad (3b)$$

$$C=\sum_{i<j}C_{ij}, \quad (3c)$$

$$D=\sum_{i}D_i. \quad (3d)$$

We omit $\tilde{C}$ and $\tilde{D}$, since these will be shown to be negligible. Also, $B_{\alpha\alpha}=\tilde{B}_{24}+\mathrm{Re}B_{24}$ and $C_{\alpha\alpha}=C_{24}$ will be found to be negligible.

In general, $B_{\pi\pi}=\tilde{B}_{13}+\mathrm{Re}B_{13}$ and $C_{\pi\pi}=C_{13}$ contribute to the cross-section average; the remaining components $B_{\pi\alpha}$ and $C_{\pi\alpha}$ contribute to the difference. The matter is less definite for the internal terminating corrections D. Assuming soft-photon dominance in these terms, we will be able to show that $D_\pi=D_1+D_3$ contributes to the average, that $D_\alpha=D_2+D_4$ contributes to the difference, and that the real internal-line bremsstrahlung D_0 is negligible. In summary, to first order,[19]

$$\frac{1}{2}\left[\frac{d\sigma^{(+)}}{d\Omega}+\frac{d\sigma^{(-)}}{d\Omega}\right]\approx\frac{4}{s}[|A_{ST}|^2(1+2\alpha B_{\pi\pi})+2\alpha\,\mathrm{Re}A_{ST}{}^*(C_{\pi\pi}+D_\pi)+\alpha^2|A_{C,B}|^2], \quad (4a)$$

$$\frac{1}{2}\left[\frac{d\sigma^{(+)}}{d\Omega}-\frac{d\sigma^{(-)}}{d\Omega}\right]\approx\frac{4}{s}[2\alpha\,\mathrm{Re}A_{ST}{}^*(A_{C,B}+B_{\pi\alpha}A_{ST}+C_{\pi\alpha}+D_\alpha)], \quad (4b)$$

where we have now removed the z_π dependence from $A_{C,B}$ and the distortion terms.

Once $B_{\pi\pi}$, $C_{\pi\pi}$, and D_π are calculated (C and D being dependent upon A_{ST}) and a strong-interaction model is chosen to fix the functional form of A_{ST}, then experimental cross-section average data can be fitted to determine the parameters in A_{ST}. (The electromagnetic contributions to the average are small, so the value chosen for r_π is not crucial here.) Then a calculation of $B_{\pi\alpha}$, $C_{\pi\alpha}$, and D_α will make it possible to determine r_π and other remaining parameters by fitting cross-section difference data.

B. Photon Terminating on External Lines (Hadrons on Shell)

As pointed out in the preceding section, the first-order electromagnetic corrections with the strong ampli-

[15] $F_\alpha(q^2)$ has been experimentally found to be Gaussian with $r_\alpha=1.66\pm0.04$ F for $0.07\leq q^2\leq5.7$ F^{-2} (1 F^{-2} corresponds to 197.32 MeV^2): R. Hofstadter, Rev. Mod. Phys. **28**, 214 (1956); H. Frank, D. Haas, and H. Prang, Phys. Letters **19**, 391 (1965).

[16] Neither theory nor experiment presently suggests what the structure of F_π may be like beyond the q^2 term, so we use the pole form rather than, for example, the exponential $\exp(-\frac{1}{6}r_\pi{}^2q^2)$.

[17] E. Corinaldesi and R. Jost, Helv. Phys. Acta **21**, 183 (1948).

[18] D. R. Yennie, S. C. Frautschi, and H. Suura, Ann. Phys. (N. Y.) **13**, 379 (1961).

[19] The squared Born term is included, since it is significant near the forward direction even though of second order in α.

tude left on shell contribute, after canceling infrared divergences, a factor $1+2\alpha(\tilde{B}+\mathrm{Re}B)$ to the cross section. In this section we compute the terms $\tilde{B}_{ij}+\mathrm{Re}B_{ij}$ and show that they can be neglected.

Using Eqs. (C4) and (C8) of Ref. 18, we can write

$$\tilde{B}_{ij}+\mathrm{Re}B_{ij}=-\frac{z_i\theta_i z_j\theta_j}{2\pi}\Bigg\{-\ln\frac{(\Delta k)^2}{E_iE_j}+\tfrac{1}{2}p_i\cdot p_j\int_{-1}^{1}\frac{dx}{p_x^{\,2}}\ln\frac{(\Delta k)^2}{E_x^{\,2}}+\tfrac{1}{4}\int_{-1}^{1}dx\ln\frac{p_x'^{\,2}}{m_im_j}+\tilde{G}_{ij}(1)+\tilde{G}_{ij}(-1)-p_i\cdot p_j$$
$$\times\int_{-1}^{1}\frac{dx}{p_x^{\,2}}\tilde{G}_{ij}(x)+\tfrac{1}{4}p_i\cdot p_j|\theta_i+\theta_j|\Bigg[\int_{-1}^{1}\frac{dx}{p_x'^{\,2}}\ln x^2+\frac{2\pi^2\theta(x_+x_-)}{[(p_i\cdot p_j)^2-m_i^2m_j^2]^{1/2}}\Bigg]\Bigg\}, \quad (5)$$

where

$$2p_x=(1+x)p_i+(1-x)p_j,\quad 2p_x'=(1+x)p_i\theta_i-(1-x)p_j\theta_j,$$
$$\tilde{G}_{ij}(x)=\frac{E_x-|\mathbf{p}_x|}{2|\mathbf{p}_x|}\ln\left(\frac{E_x+|\mathbf{p}_x|}{E_x-|\mathbf{p}_x|}\right)+\ln\left(\frac{E_x+|\mathbf{p}_x|}{2E_x}\right),$$
$$x_\pm=\frac{-(m_i^2-m_j^2)\pm2[(p_i\cdot p_j)^2-m_i^2m_j^2]^{1/2}}{m_i^2+m_j^2+2p_i\cdot p_j},$$

$\theta_i=+1$ if the ith particle is outgoing, -1 if incoming, and Δk is the minimum detectable infrared photon three-momentum (about 2 MeV/c for the Berkeley experiment[20]).

In the low-energy limit $k\ll m_\pi$, it is simply a matter of algebra to show that the contributions to the cross-section average $B_{\pi\pi}$ and $B_{\alpha\alpha}$ are of order

$$B_{\pi\pi}\approx k^2/m_\pi^{\,2}\quad\text{and}\quad B_{\alpha\alpha}\approx B_{\pi\pi}(m_\pi/m_\alpha)\quad\text{for } k\ll m_\pi. \quad (6)$$

It is immediately clear that $B_{\alpha\alpha}$ can be neglected in comparison with $B_{\pi\pi}$.

At higher momenta it is easier to simply do the integrals numerically. This is also true for the contributions to the cross-section difference

$$B_{\pi\alpha}=2(\tilde{B}_{12}+\mathrm{Re}B_{12})+2(\tilde{B}_{14}+\mathrm{Re}B_{14}). \quad (7)$$

Some values of $2\alpha(\tilde{B}_{ij}+\mathrm{Re}B_{ij})$ for angles near which A_{ST} is a minimum[21] are given in Table III.

From these results, it is evident that in all these cases $2\alpha(\tilde{B}_{ij}+\mathrm{Re}B_{ij})$ is of the order of 0.01 or less. We shall see later that the total distortion amplitude, including the C_{ij} and D_i terms, is in the order of 10% of A_{ST}.

TABLE III. Values of the on-shell electromagnetic correction factors $2\alpha(\tilde{B}_{ij}+\mathrm{Re}B_{ij})$ for $\pi^\pm\alpha$ scattering near the strong-interaction minimum.

(i,j)	$T^{\mathrm{lab}}=24$ MeV $\theta_{\mathrm{c.m.}}=76.9°$	$T^{\mathrm{lab}}=51$ MeV $\theta_{\mathrm{c.m.}}=72.7°$	$T^{\mathrm{lab}}=75$ MeV $\theta_{\mathrm{c.m.}}=73.0°$
(1,3)	0.00345	0.00680	0.01012
(2,4)	0.00004	0.00007	0.00012
(1,2)	0.00128	−0.00501	−0.01023
(1,4)	−0.00540	−0.00021	0.00482

[20] K. M. Crowe (private communication).

[21] The effects of distortion upon r_π are most pronounced in this region, which is where the Born Coulomb term, which dominates the forward direction, competes with the distortion terms, which dominate the backward direction.

Thus $B_{\pi\pi}$ and $B_{\pi\alpha}$ turn out to be only a small part of the total distortion.

C. Photon Terminating on External Lines (Hadrons off Shell)

Next we turn to the off-shell parts of the external terminating diagrams. Letting $\{p_i\}$ be the set of on-shell momenta, $p_i^{\,2}=m_i^{\,2}$, we write these corrections in terms of the difference

$$A_{ST}(p_1',p_2',p_3',p_4')-A_{ST}(p_1,p_2,p_3,p_4),$$

where the momenta $\{p_i'\}$ are off shell and A_{ST} is the strong amplitude written in a form which permits us to take the momenta off shell.

1. Virtual Photons

The electromagnetic corrections involving one virtual photon with both ends terminating on a line external to the strong-interaction subdiagram are shown in Fig. 4. In those diagrams in which both ends terminate on the same line, the strong amplitude A_{ST} is on shell. In those in which the virtual photon connects two different

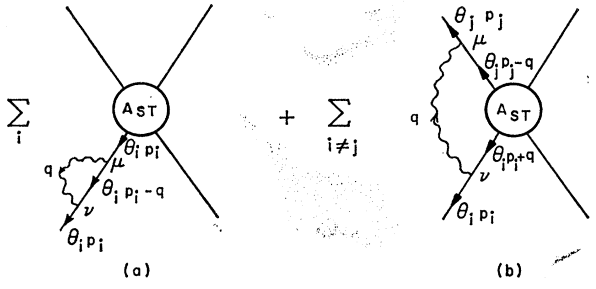

FIG. 4. Virtual photon terminating outside A_{ST}.

external lines, A_{ST} is off shell. Explicitly,

$$A_{ij}^{(b)}=4\pi i\alpha\theta_i z_i\theta_j z_j\int\frac{d^4q}{(2\pi)^4q^2}\times\frac{(2\theta_i p_i+q)\cdot(2\theta_j p_j-q)}{[(\theta_i p_i+q)^2-m_i^2][(\theta_j p_j-q)^2-m_j^2]}\times A_{ST}(p_i\to p_i+\theta_i q,\ p_j\to p_j-\theta_j q). \quad (8)$$

Now we add and subtract the on-shell A_{ST} inside the integral. The on-shell term, together with the Fig. 4(a) diagrams, gives us the standard infrared correction[19]

$$B=\sum_{i<j}B_{ij}, \quad (9)$$

where

$$B_{ij}=-\frac{i}{8\pi^3}\theta_i z_i\theta_j z_j\int\frac{d^4q}{q^2}\times\left[\frac{(2p_i\theta_i-q)_\mu}{q^2-2q\cdot p_i\theta_i}+\frac{(2p_j\theta_j+q)_\mu}{q^2+2q\cdot p_j\theta_j}\right]^2. \quad (10)$$

The remainder, which we denoted above by C, is the correction due to the off-shell behavior of the amplitude. It is given by

$$\alpha C=\alpha\sum_{i\neq j}C_{ij}, \quad (11)$$

where

$$C_{ij}=\frac{i}{4\pi^3}\theta_i z_i\theta_j z_j\int\frac{d^4q}{q^2}\frac{(2\theta_i p_i+q)\cdot(2\theta_j p_j-q)}{(q^2+2q\cdot p_i\theta_i)(q^2-2q\cdot p_j\theta_j)}\times[A_{ST}(p_i\to p_i+\theta_i q,\ p_j\to p_j-\theta_j q)-A_{ST}]. \quad (12)$$

Of course, this assumes point Coulomb interactions, so to be correct we must insert the appropriate form factors $F_i(q^2,\theta_i q\cdot p_i)$ before integrating. For the α particle this can be taken as simply $F_\alpha(q^2)$, since we assume external α legs remain approximately on-shell. However, here we must consider all q^2, even large timelike values. The form $\exp(-\frac{1}{6}r_\alpha^2q^2)$ runs into difficulty for large negative q^2. So (to assure convergnece), rather than the Gaussian, we will use the pole form

$$F_\alpha(q^2)\approx 1/(1+\tfrac{1}{6}r_\alpha^2q^2). \quad (13)$$

For the $\pi\pi\gamma$ vertex with one pion off shell (as well as the photon) we assume that for the momenta of interest it is approximately given by the on-shell value,[22]

$$-ie\{F(q^2,q\cdot p)(2p-q)_\mu+[(q^2-2q\cdot p)/q^2](F(q^2,q\cdot p)-1)q_\mu\}\approx -ieF_\pi(q^2)(2p-q)_\mu. \quad (14)$$

The amplitude A_{ST} with pion legs off shell is derived in Sec. III A. Using the expansion to second order in momenta, we have

$$C_{21}=-\frac{iz_\pi\theta_1\theta_2}{32\pi^4}\int\frac{d^4q}{q^2}\frac{-2B_s q\cdot p_3+C_s[q^2-2q\cdot(p_1-p_3)]}{(q^2+2q\cdot p_2)(q^2-2q\cdot p_1)}\times F_\alpha(q^2)(2p_2+q)^\mu F_\pi(q^2)(2p_1-q)_\mu, \quad (15a)$$

$$C_{31}=-\frac{i}{64\pi^4}\int\frac{d^4q}{q^2}\frac{2B_s[q^2-q\cdot(p_1+p_3)]}{(q^2-2q\cdot p_3)(q^2-2q\cdot p_1)}\times F_\pi(q^2)(2p_1-q)^\mu F_\pi(q^2)(2p_3-q)_\mu. \quad (15b)$$

Thus, using $C_{23}=C_{21}(p_2\leftrightarrow -p_4)$, we can compute $C_{\pi\alpha}=2(C_{21}+C_{23})$ and $C_{\pi\pi}=C_{31}$.[23] To calculate C_{21}, we define

$$P\equiv -2B_s p_3-2C_s(p_1-p_3), \quad (16)$$

$$Q\equiv 2(p_1-p_2), \quad (17)$$

$$M_{\pi,\alpha}^2\equiv 6/r_{\pi,\alpha}^2. \quad (18)$$

Then

$$C_{21}=-\frac{iz_\pi}{32\pi^4}M_\pi^2M_\alpha^2\int\frac{d^4q}{q^2}\frac{4(p_1\cdot p_2)q\cdot P+(q\cdot P)(q\cdot Q)+4C_s(p_1\cdot p_2)q^2+q^2q\cdot(C_sQ-P)-C_sq^4}{q^2(M_\pi^2+q^2)(M_\alpha^2+q^2)(q^2+2q\cdot p_2)(q^2-2q\cdot p_1)}, \quad (19)$$

$$=\frac{z_\pi}{32\pi^2}M_\alpha^2\int_0^1dx\int_0^x dy\left\{[4(p_1\cdot p_2)(g\cdot P)+(g\cdot P)(g\cdot Q)]\left[\frac{1}{M_\alpha^2}\left(\frac{1}{-g^2}-\frac{1}{-g^2+yM_\alpha^2}\right)+\frac{1}{M_\pi^2-M_\alpha^2}\left(\frac{1}{-g^2+yM_\pi^2}-\frac{1}{-g^2+yM_\alpha^2}\right)\right]+\frac{M_\pi^2}{M_\alpha^2-M_\pi^2}\left[[4C_s(p_1\cdot p_2)+g\cdot(C_sQ-P)-C_sg^2]\times\left(\frac{1}{-g^2+yM_\pi^2}-\frac{1}{-g^2+yM_\alpha^2}\right)+2C_s\ln\frac{-g^2+yM_\pi^2}{-g^2+yM_\alpha^2}\right]\right\}, \quad (20)$$

[22] The form of the left-hand side follows from Lorentz invariance and Ward's identity. Note that the right-hand side involves two assumptions: that $F(q^2,q\cdot p)\approx F_\pi(q^2)$ and that the q_μ contribution is negligible. (If we included the q_μ term, it would be necessary to dampen A_{ST} at high momenta to overcome an ultraviolet divergence.)

[23] Strictly speaking, when calculating C_{23} and C_{31} it is necessary to use the values of B_s and C_s corresponding to $s=(p_1+p_2-q)^2$ rather than $s=(p_1+p_2)^2$. However, we assume B_s and C_s are slowly varying over the range of q dominating the integral (cf. Table V).

where

$$g\equiv(1-x)p_1+(y-x)p_2. \tag{21}$$

Numerical calculation of the double integral for typical values of the parameters shows that $C_{\pi\alpha}$ is in the order of 10% of $A_{\rm ST}$.[24] This (together with D_α to be computed in Sec. II D) contains the bulk of the distortion effects in the cross-section difference.

2. Real Photons

In this section, we show that the off-shell contribution of the real photon correction is of the order

$$\sum_{\pm}\int^{\omega_q<\Delta E}\frac{d^3q}{(2\pi)^4 2\omega_q}|\tilde{C}|^2\lesssim\frac{32\alpha}{\pi}\frac{\Delta k}{m_\pi}\frac{k^2}{t}\left(1-\frac{m_\pi\Delta k}{t}\right)\times|A_{\rm ST}+O(m_\alpha a_L)|^2, \tag{22}$$

where $\Delta k=\Delta E$ is the experimental limit of resolution and a_L is the $\pi^0\alpha$ scattering length. In the experiments conducted to date, $|t|>\frac{1}{4}m_\pi^2$ and $\Delta k\approx 2$ MeV/c. Under these circumstances, the real photon contributions are negligible. (So long as $\Delta k<5$ MeV/c, these contributions make up less than 1% of the total cross section.)

The real external terminating corrections (Fig. 5), in which the photon carries off energy $\omega_q<\Delta E$, are not coherent with the virtual photon corrections because of the additional external line.

Let us write the amplitude for these processes as

$$A_\pm'=\sum_i(A_\pm')_i, \tag{23}$$

where[25]

$$(A_\pm')_i=-e\theta_i z_i\frac{(2\theta_i p_i+q)_\mu\epsilon_\pm^\mu(\hat{q})}{2\theta_i p_i\cdot q}\times A_{\rm ST}(p_i\to p_i+\theta_i q). \tag{24}$$

The second term in the numerator vanishes, since $q_\mu\epsilon_\pm^\mu(\hat{q})=0$.

We use the trick of breaking this up into on-shell and off-shell parts:

$$(A_\pm')_i=(A_\pm')_i^{(\rm on)}+(A_\pm')_i^{(\rm off)}, \tag{25}$$

where

$$(A_\pm')_i^{(\rm on)}=-e\theta_i z_i\frac{p_i\cdot\epsilon_\pm(\hat{q})}{p_i\cdot q}A_{\rm ST}, \tag{26}$$

$$(A_\pm')_i^{(\rm off)}=-e\theta_i z_i\frac{p_i\cdot\epsilon_\pm(\hat{q})}{p_i\cdot q}\times[A_{\rm ST}(p_i\to p_i+\theta_i q)-A_{\rm ST}]. \tag{27}$$

[24] The double numerical integration also shows that the $C_s q^4$ term can be neglected. This is of practical importance, since the y integration for the other terms can be done analytically, leaving only the x integration to be done numerically when curve fitting.

[25] The photon polarization vector can be written

$$\epsilon_\pm^\mu(\hat{q}(\theta,\phi))=\frac{1}{\sqrt{2}}\left(0,\frac{\pm\cos\theta-i\sin^2\theta\cos\phi\sin\phi}{\cos^2\theta+\sin^2\theta\cos^2\phi},-i,\frac{\sin\theta(\pm\cos\phi+i\cos\theta\sin\phi)}{\cos^2\theta+\sin^2\theta\cos^2\phi}\right).$$

FIG. 5. Real photon terminating outside $A_{\rm ST}$.

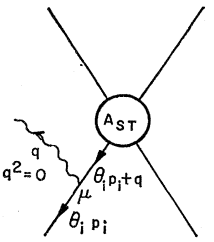

If we look at $(A_\pm')_i^{(\rm on)}$ alone and compute its contribution to the cross section, we obtain the standard infrared correction[19]

$$\tilde{B}=\sum_{i<j}\tilde{B}_{ij}, \tag{3b}$$

where

$$\tilde{B}_{ij}=\frac{1}{8\pi^2}\theta_i z_i\theta_j z_j\sum_\pm\int^{\omega_q<\Delta E}\frac{d^3q}{(|\mathbf{q}|^2+\lambda^2)^{1/2}}\times\left|\frac{p_i\cdot\epsilon_\pm(\hat{q})}{p_i\cdot q}-\frac{p_j\cdot\epsilon_\pm(\hat{q})}{p_j\cdot q}\right|^2. \tag{28}$$

The off-shell-dependent remainder is

$$\sum_\pm\int^{\omega_q\Delta E}\frac{d^3q}{(2\pi)^3\omega_q}\{|\sum_i(A_\pm')_i^{(\rm off)}|^2+2\,{\rm Re}[\sum_i(A_\pm')_i^{(\rm off)*}\cdot\sum_j(A_\pm')_j^{(\rm on)}]\}. \tag{29}$$

Thus the off-shell contributions due to real infrared photons of momenta less than $\Delta k=\Delta E$ are (using the $A_{\rm ST}$ given in Sec. III A) related to (dropping q^2 compared with $q\cdot p_{1,3}$)

$$\sum_i(A_\pm')_i^{(\rm off)}\approx\frac{ez_\pi}{8\pi}\left[B_s q\cdot\left(p_3\frac{p_1\cdot\epsilon_\pm}{p_1\cdot q}+p_1\frac{p_3\cdot\epsilon_\pm}{p_3\cdot q}\right)+C_s q\cdot(p_1-p_3)\left(\frac{p_1\cdot\epsilon_\pm}{p_1\cdot q}-\frac{p_3\cdot\epsilon_\pm}{p_3\cdot q}\right)\right], \tag{30}$$

while the on-shell contributions come from

$$\sum_i(A_\pm')_i^{(\rm on)}=ez_\pi\left(\frac{p_1\cdot\epsilon_\pm}{p_1\cdot q}-\frac{p_3\cdot\epsilon_\pm}{p_3\cdot q}\right)A_{\rm ST}. \tag{31}$$

Since $(A_\pm')_3=(A_\pm')_1(p_3\leftrightarrow -p_1)$, it is sufficient to consider only the $p_1\cdot\epsilon_\pm$ terms. Further, observe that when we compute $|A'^{(\rm off)}|^2+2\,{\rm Re}(A'^{(\rm off)*}A'^{(\rm on)})$, we will have terms of the form $1+p_3\cdot q/p_1\cdot q$ or $1+p_1\cdot q/p_3\cdot q$. Now $\omega_1=\omega_3$ and $|\mathbf{p}_1|=|\mathbf{p}_3|$. Thus, for purposes of magnitude estimation we will assume $p_3\cdot q/p_1\cdot q$ is of order unity, and so neglecting it will not decrease the order of

magnitude of the result. Therefore

$$|A_\pm'^{(\mathrm{off})}|^2 \approx (\alpha/16\pi)|C_s(p_1\cdot\epsilon_\pm)|^2, \quad (32)$$

$$A_\pm'^{(\mathrm{off})*}A_\pm'^{(\mathrm{on})} \approx \tfrac{1}{2}\alpha\frac{|(p_1\cdot\epsilon_\pm)|^2}{p_1\cdot q}C_s^*A_{\mathrm{ST}}. \quad (33)$$

Since $|A\cdot\epsilon_\pm| \leq |\mathbf{A}|$, this gives the upper bounds

$$|A_\pm'^{(\mathrm{off})}| \lesssim (\alpha/16\pi)|C_s|^2k^2, \quad (34)$$

$$|A_\pm'^{(\mathrm{off})*}A_\pm'^{(\mathrm{on})}| \lesssim \frac{\alpha}{32\pi}\frac{k^2}{|p_3\cdot q|} \times|C_s^*[(2B_s-C_s)m_\pi^2-(B_s-C_s)t]|. \quad (35)$$

For the first term in (29), the integral is simply

$$\int^{\omega_q<\Delta E}\frac{d^3q}{(2\pi)^3\omega_q} = \frac{4\pi}{(2\pi)^3}\tfrac{1}{2}(\Delta k)^2. \quad (36)$$

For the second term it is

$$\int^{\omega_q<\Delta E}\frac{d^3q}{(2\pi)^3\omega_q}\frac{1}{p_3\cdot q} = -\frac{1}{(2\pi)^2}\frac{\Delta k}{k}\ln\frac{\omega-k}{\omega+k} \quad (37)$$

$$\approx \frac{2}{(2\pi)^2}\frac{\Delta k}{m_\pi} \quad \text{for} \quad k\ll m_\pi. \quad (38)$$

Thus the contributions to the cross section, doing the sum $\sum_\pm$, are of the orders

$$\lesssim[2\alpha/(4\pi)^3](\Delta k)^2k^2|C_s|^2 \quad (39)$$

and

$$\lesssim[4\alpha/(4\pi)^3](\Delta k/m_\pi)k^2|C_s^*[(2B_s-C_s)m_\pi^2 -(B_s-C_s)t]|. \quad (40)$$

Finally, to obtain the desired result, Eq. (22), we add Eqs. (39) and (40) and use the relation

$$A_{\mathrm{ST}} \approx m_\alpha a_L - (m_\alpha a_L/2m_\pi^2 + C_s/32\pi)t, \quad (41)$$

to be derived in Sec. III A.

D. Photon Terminating on Internal Lines

1. Virtual Photons

Consider the off-shell amplitude $A_\mu^n(p_1,p_2,p_3,p_4,q)$ in which one virtual photon of momentum q and polarization μ is emitted either by an external line ($n=1,2,3,4$) or an internal line ($n=0$). For $n=1, 2, 3, 4$ we can calculate explicitly (using the exact $\pi\pi\gamma$ and $\alpha\alpha\gamma$ vertices with one hadron off shell)

$$q^\mu A_\mu^n(p_1,p_2,p_3,p_4,q) = z_n e q^\mu[F_n(q^2,-\theta_n q\cdot p_n)(2p_n+\theta_n q)_\mu + G_n(q^2,-\theta_n q\cdot p)q_\mu]\frac{A_{\mathrm{ST}}(p_n\to p_n+\theta_n q)}{(p_n+\theta_n q)^2-m_n^2} \quad (42)$$

$$= z_n e q\cdot(2p_n+\theta_n q)\frac{A_{\mathrm{ST}}(p_n\to p_n+\theta_n q)}{(p_n+\theta_n q)^2-m_n^2}, \quad (43)$$

where $z_n e$ is the charge of the nth line.

Defining

$$A_\mu = \sum_{n=0}^{4} A_\mu^n,$$

we will know $q^\mu A_\mu^0$ if we know $q^\mu A_\mu$. When all the external lines excluding the added photon are on shell, $p_n^2=m_n^2$, $n=1, 2, 3, 4$, current conservation tells us that $q^\mu A_\mu=0$. However, we need $q^\mu A_\mu$ with off-shell hadrons. This is given by off-shell current conservation expressed in the generalized Ward identity[26]

$$q^\mu A_\mu(p_1,p_2,p_3,p_4,q) = z_\pi e\left[\frac{(p_1^2-m_\pi^2)A_{\mathrm{ST}}(p_1-q,p_2,p_3,p_4)}{(p_1-q)^2-m_\pi^2} - \frac{(p_3^2-m_\pi^2)A_{\mathrm{ST}}(p_1,p_2,p_3+q,p_4)}{(p_3+q)^2-m_\pi^2}\right] + z_\alpha e\left[\frac{(p_2^2-m_\alpha^2)A_{\mathrm{ST}}(p_1,p_2-q,p_3,p_4)}{(p_2-q)^2-m_\alpha^2} - \frac{(p_4^2-m_\alpha^2)A_{\mathrm{ST}}(p_1,p_2,p_3,p_4+q)}{(p_4+q)^2-m_\alpha^2}\right]. \quad (44)$$

Therefore

$$q^\mu A_\mu^0 = z_\pi e[A_{\mathrm{ST}}(p_1-q)-A_{\mathrm{ST}}(p_3+q)] + z_\alpha e[A_{\mathrm{ST}}(p_2-q)-A_{\mathrm{ST}}(p_4+q)]. \quad (45)$$

Leaving the external α particles on shell and taking A_{ST} to second order in the momenta, we have

$$q^\mu A_\mu^0 = (z_\pi e/8\pi)B_s q\cdot(p_1+p_3). \quad (46)$$

From this it follows that the amplitude for Fig. 3(f), permitting the photon and the pions to go off shell, is

$$A_\mu^0 = (z_\pi e/8\pi)B_s(p_1+p_3)_\mu + R_\mu, \quad (47)$$

where the remainder satisfies $R_\mu q^\mu=0$, i.e., given any four-vector V_ν we can construct $R_\mu=(g_{\mu\nu}-q_\mu q_\nu/q^2)V^\nu$. However, bremsstrahlung from internal lines produces no infrared divergences, so A_μ^0 is not singular as $q\to 0$. Hence R_μ is of order q.[27] So for soft photons,

$$A_\mu^0 \approx (z_\pi e/8\pi)B_s(p_1+p_3)_\mu \quad \text{for} \quad |q^2|\ll m_\pi^2. \quad (48)$$

[26] E. Kazes, Nuovo Cimento **13**, 1226 (1959). Although the identity is proved only for Feynman diagrams involving spin-0 and spin-$\frac{1}{2}$ particles (as well as the photon), we assume it to be true for elastic $\pi\alpha$ scattering whatever intermediate states may be involved.

[27] See F. E. Low, Phys. Rev. **110**, 974 (1958); E. M. Nyman, *ibid.* **170**, 1628 (1968). This argument of course fails for external terminating photons, so we could not determine A_μ^i from $q^\mu A_\mu^i$ for $i=1, 2, 3, 4$. [The leading terms for the next order in e are examined by T. P. Cheng, *ibid.* **176**, 1674 (1968).]

Denoting by αD_π the contributions of Figs. 3(a) and 3(b), and by αD_α the contributions of Figs. 3(c) and 3(d), we have

$$\alpha D_{\pi(\alpha)}=-iez_{\pi(\alpha)}\int\frac{d^4q}{(2\pi)^4q^2}\times\left[\frac{(2p_{1(2)}+q)^\mu A_\mu{}^0(p_{1(2)}\to p_{1(2)}+q)}{(p_{1(2)}+q)^2-m_{\pi(\alpha)}{}^2}F_{1(2)}(q^2)+\frac{(2p_{3(4)}-q)^\mu A_\mu{}^0(p_{3(4)}\to p_{3(4)}-q)}{(p_{3(4)}-q)^2-m_{\pi(\alpha)}{}^2}F_{3(4)}(q^2)\right]. \quad (49)$$

This formula shows that we do not need to know $A_\mu{}^0$ completely. We only need $q^\mu A_\mu{}^0$ and $p^\mu A_\mu{}^0$, the first of which we already know. To get the second we would need two more independent scalar constraints on $A_\mu{}^0$, i.e., we would need to know $A_\mu{}^0$ up to one scalar constraint.

If we assume that the soft-photon ($q^2\ll m_\pi{}^2$) part of the integral dominates, we can caclulate the $p_i{}^\mu A_\mu{}^0$ terms completely. In this case, D_π is proportional to z_π and hence contributes only to the cross-section average. (We will find later that all radiative corrections to the average are small.) However, if the hard-photon part is significant, D_π may contribute an important part to the cross-section difference, which we could not calculate here even if we knew the off-shell $\pi^0\alpha$ elastic amplitude exactly. If we separate the hard-photon part of $A_\mu{}^0$ into a part which depends on z_π and a part which does not, we get

$$A_\mu{}^0=A_\mu{}^0|_{\text{soft}}+B_\mu{}^0(z_\pi)+C_\mu{}^0, \quad (50)$$

where $B_\mu{}^0(z_\pi)$ and $C_\mu{}^0$ are of order q; the omitted contributions to the cross-section difference come from the terms

$$C_\mu{}^0 p_{1,3}{}^\mu \quad (51a)$$

and

$$B_\mu{}^0(z_\pi)p_{2,3}{}^\mu \quad (51b)$$

in D_π and D_α, respectively.

If we make the soft-photon dominance assumption for $p_s{}^\mu A_\mu{}^0$, our second-order expression for D_α becomes

$$D_\alpha=-\frac{i}{(2\pi)^4}B_s(p_1+p_3)_\mu\int\frac{d^4q}{q^2}F_\alpha(q^2)\times\left[\frac{(2p_2+q)^\mu}{q^2+2q\cdot p_2}+\frac{(2p_4-q)^\mu}{q^2-2q\cdot p_4}\right]. \quad (52)$$

If we take $F_\alpha(q^2)\approx 1/(1+\frac{1}{6}r_\alpha{}^2q^2)$, the integral can be done easily, giving

$$D_\alpha=\frac{\pi B_s}{(2\pi)^4}(s-u)\int_0^1 dx(1+x)\times\ln\left[1-\frac{6x}{(1-x)^2(r_\alpha m_\alpha)^2}\right] \quad (53)$$

$$=-\frac{0.056}{\pi^2}\frac{s-u}{t}\left[A_{\text{ST}}-m_\alpha a_L\left(1-\frac{t}{m_\pi{}^2}\right)\right], \quad (54)$$

where we have used $r_\alpha m_\alpha=31.4$ and the approximation

$$A_{\text{ST}}\approx m_\alpha a_L-(m_\alpha a_L/m_\pi{}^2+B_s/16\pi)t, \quad (55)$$

to be derived in Sec. III A.

To calculate the contribution of Fig. 3(c), where both ends of the virtual photon terminate on internal lines, we simply reiterate the use of Ward's identity. Let $A_{\mu\nu}{}^{0m}(p_1,p_2,p_3,p_4,q,q')$ be the amplitude $A_\mu{}^0$, with an additional photon of momentum q' and polarization ν inserted in line m. Following the same procedure as before, we get

$$q^\nu A_{\mu\nu}{}^{00}=z_\pi e[A_\mu{}^0(p_1-q')-A_\mu{}^0(p_3+q')]+z_\alpha e[A_\mu{}^0(p_2-q')-A_\mu{}^0(p_4+q')]. \quad (56)$$

Putting the α particles on shell and taking the soft-photon limit, we have

$$q^\nu A_{\mu\nu}{}^{00}\approx-\alpha B_s q_\mu'. \quad (57)$$

From the nonsingularity of $A_{\mu\nu}{}^{00}$ as $q'\to 0$, we have

$$A_{\mu\nu}{}^{00}=-\alpha B_s+O(q,q'). \quad (58)$$

The desired amplitude is now obtained by setting $q'=-q$, inserting the photon propagator, and integrating over the photon momentum. However, the integrand depends only on q^2, so the integral vanishes because of spherical symmetry of the kernel

$$\alpha D_0=0. \quad (59)$$

Here also we have omitted the hard-photon contribution, the full term being of the form

$$\alpha D_0=\alpha D_0|_{\text{soft}}-i\int\frac{d^4q}{(2\pi)^4q^2}\times F_\pi F_\pi g^{\mu\nu}[B_{\mu\nu}{}^{00}(z_\pi)+C_{\mu\nu}{}^{00}], \quad (60)$$

where the unknown terms $B_{\mu\nu}{}^{00}(z_\pi)$ and $C_{\mu\nu}{}^{00}$ are of first order in $q=-q'$, and contribute to the cross-section difference and average, respectively.

2. Real Photons

The amplitude for emission of a real photon from an internal line [Fig. 3(f)] is simply

$$A_\mu{}^0\epsilon^{\mu\pm}=(ez_\pi/8\pi)(B_s-2C_s)(p_1-p_3)_\mu\epsilon^{\mu\pm}, \quad (61)$$

where we can neglect terms $O(q)$ because we restrict the integral to infrared photons. The contribution which this term alone makes to the average cross section is

$$\sum_\pm\int^{\omega_q<\Delta E}\frac{d^3q}{(2\pi)^3\omega_q}|A_\mu{}^0\epsilon^{\mu\pm}|^2\lesssim\frac{4\alpha}{(4\pi)^3}(\Delta k)^2\times|B_s-2C_s|^2k^2(1-\cos\theta), \quad (62)$$

which is of the same order of magnitude as the real photon contribution from external lines, hence negligible.

III. STRONG $\pi\alpha$ SCATTERING: LOW-ENERGY $\pi\alpha$ ELASTIC AMPLITUDE WITH EXTERNAL PIONS OFF SHELL

The invariant $\pi\alpha \to \pi\alpha$ amplitude $\mathfrak{M}$ (see Fig. 6) with both pions off shell is defined by[28]

$$i\mathfrak{M}(\alpha(p_4),\pi_\beta(p_3);\alpha(p_2),\pi_\alpha(p_1))c_\pi m_\pi^2 a_\pi$$
$$=(m_\pi^2-p_3^2)(m_\pi^2-p_1^2)\int d^4x\, e^{-ip_1\cdot x}$$
$$\times\langle\alpha(p_4)|T(\partial_\mu A_\alpha{}^\mu(x)v_\beta(0))|\alpha(p_2)\rangle, \quad (63)$$

where $p_2^2=p_4^2=m_\alpha^2$, v is the pseudoscalar field, a_π is the v-field normalization constant $\langle 0|v_\alpha(0)|\pi_\beta(p)\rangle = a_\pi\delta_{\alpha\beta}$ (so v is related to the pion field ϕ by $v=a_\pi\phi$), A^μ is the axial-vector current, and c_π is the PCAC proportionality constant $\partial_\mu A^\mu = c_\pi m_\pi^2\phi$. Also, $a_\pi = c_\pi m_\pi^2$ and $c_\pi = m_N g^A/G_{\pi NN}\approx 0.60 m_\pi$.

We now integrate by parts, and use the equal-time commutation relation

$$[Q_\alpha{}^A, v_\beta(0)] = i\delta_{\alpha\beta}\sigma(0), \quad (64)$$

where

$$Q_\alpha{}^A = \int d^4x\, A_\alpha{}^0(x)\delta(x_0), \quad (65)$$

$$\sigma(x) = (\sqrt{\tfrac{2}{3}})u_0 + (\sqrt{\tfrac{1}{3}})u_8, \quad (66)$$

and u is the scalar field. Then, going to the limit of small p_1,[29] we have

$$\lim_{p_1\to 0}\mathfrak{M}(\alpha(p_4),\pi_\beta(p_3);\alpha(p_2),\pi_\alpha(p_1))$$
$$=-m_\pi^2(m_\pi^2-p_3^2)\langle\alpha(p_4)|\sigma(0)|\alpha(p_2)\rangle$$
$$\times(\delta_{\alpha\beta}/c_\pi m_\pi^2 a_\pi). \quad (67)$$

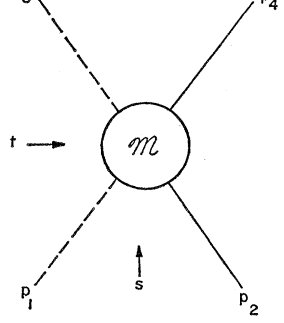

FIG. 6. $\pi\alpha$ nuclear amplitude.

The matrix element $\langle\alpha|\sigma|\alpha\rangle$ is just the $\sigma\alpha\alpha$ vertex

$$\langle\alpha(p_4)|\sigma(0)|\alpha(p_2)\rangle = F_{\sigma\alpha\alpha}(p_4^2,p_2^2,(p_4-p_2)^2), \quad (68)$$

which gives, at threshold ($s=h=\sum_i m_i^2$, $t=u=0$), the coupling constant

$$G_{\sigma\alpha\alpha} = F_{\sigma\alpha\alpha}(m_\alpha^2,m_\alpha^2,0). \quad (69)$$

Because the α particle is an isosinglet, we may write[30]

$$\mathfrak{M}(\alpha(p_4),\pi_\beta(p_3);\alpha(p_2),\pi_\alpha(p_1))$$
$$=M(s,t,u;p_1^2,p_2^2,p_3^2,p_4^2)\delta_{\alpha\beta}. \quad (70)$$

Keeping the external α particles on shell, suppose we take $s+u$, $s-u$, $p_1^2+p_3^2$, and $p_1^2-p_3^2$ as independent variables in terms of which we expand M. Then crossing symmetry ($s\leftrightarrow u$, $p_1^2\leftrightarrow p_3^2$) says that in first order the $s-u$ and $p_1^2-p_3^2$ terms are absent. (More generally, the crossing-symmetric expansion can be immediately written to any order by taking t, $p_1^2+p_3^2$, su, and $p_1^2p_3^2$ as the independent variables.) Thus, to second order in the momenta,[31] we have

$$M = a+bt+c(p_1^2+p_3^2) \quad (71)$$
$$\xrightarrow[p_1\to 0]{} a+(b+c)p_3^2. \quad (72)$$

Equating this to our previous result as $p_1\to 0$, we obtain

$$M(m_\alpha^2,t,m_\alpha^2;0,m_\alpha^2,t,m_\alpha^2)$$
$$=-\frac{m_\pi^2-p_3^2}{c_\pi a_\pi}F_{\sigma\alpha\alpha}(m_\alpha^2,m_\alpha^2,t), \quad (73)$$

and assuming that $F_{\sigma\alpha\alpha}(m_\alpha^2,m_\alpha^2,t)\approx G_{\sigma\alpha\alpha}$ for small t,[32] we have $a=-m_\pi^2(b+c)$. Thus, redefining the constants, we get

$$M\approx 2B_s p_1\cdot p_3 + C_s(t-m_\pi^2). \quad (74)$$

Unlike the case of $\pi\pi$ scattering, here we do not have an additional relation to reduce further the number of constants. On the mass shell this becomes

$$M = -(C_s-2B_s)m_\pi^2 + (C_s-B_s)t, \quad (75)$$

[28] That this is a valid off-shell definition is shown by the LSZ formalism, which demonstrates that it approaches the on-shell amplitude as $p_{1,3}{}^2\to m_\pi^2$: H. Lehmann, K. Symanzik, and W. Zimmerman, Nuovo Cimento **1**, 205 (1955).

[29] In general, as p_1 and $p_3\to 0$, $M_{\beta\alpha}\to M_{\beta\alpha}{}^{(0)} - 2(g_V/c_\pi)^2 \times p_1\cdot p_2(T_\pi)_{\beta\alpha}(T_\alpha)+\text{poles}+O(p_1^2,p_1p_3,p_3^2)$, where $M^{(0)}$ is proportional to $F_{\sigma\alpha\alpha}$: S. Weinberg, Phys. Rev. Letters **17**, 616 (1966); A. P. Balachandran *et al.*, in Proceedings of the Conference on Particle Physics, Boulder, Colo., 1966 (unpublished). Because the α particle is an isoscalar, if the σ-type terms are omitted, the scattering length is zero, since the charge commutator gives an antisymmetric contribution to $M_{\beta\alpha}$.

[30] In the notation used previously, $M=-16\pi A_{ST}$, where $S=1+2(2\pi)^5 iA_{ST}\delta(p_i-p_f)$, so $S=1-4\pi^4 iM\delta(p_i-p_f)$.

[31] Ordinarily the problem of s-channel poles would have to be considered in going beyond the zeroth-order term. However, here crossing symmetry says that the s dependence must appear in the form of an su dependence, so the question of s-channel poles does not arise till we carry the expansion to fourth order in the momenta. It is this fortunate circumstance which permits us to say anything at all about the off-shell amplitude.

[32] See N. N. Khuri, Phys. Rev. **153**, 1482 (1967). For small t, $F(m_\alpha^2,m_\alpha^2,t)\approx G_{\sigma\alpha\alpha}[1-J_\sigma(m_\pi^2-t)]$, where $J_\sigma\approx a_L/6\pi m_\alpha$, the scattering length being given by $m_\alpha a_L = A_{ST}(\text{threshold})$. This induces a correction which is negligible for small scattering lengths.

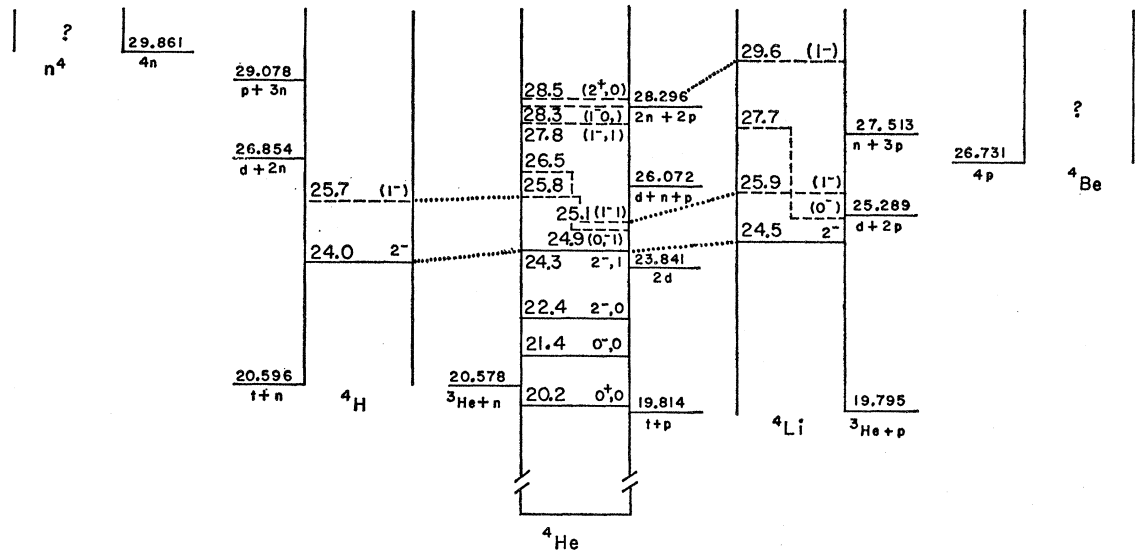

FIG. 7. Isobar diagram, $A=4$. All energies are plotted vertically in MeV and referred to the mass of ^{4}He without taking into account the neutron-proton mass difference of the Coulomb energy. Values of total angular momentum J, parity, and isobaric spin T which appear to be reasonably well established are indicated on the levels; less certain assignments are enclosed in parentheses. Levels which are presumed to be isospin multiplets are connected by dotted lines. Two possible arrangements of the $T=1$ levels are shown. [Reproduced from W. E. Meyerhof and T. A. Tombrello, Nucl. Phys. **A109**, 39 (1968).]

which gives

$$A_{ST}\approx m_\alpha a_L-(m_\alpha a_L/m_\pi^2+B_s/16\pi)t \tag{55}$$

$$=m_\alpha a_L-\tfrac{1}{2}(m_\alpha a_L/m_\pi^2+C_s/16\pi)t. \tag{41}$$

The expansion of M to second order in momenta is equivalent to an off-shell partial-wave expansion for $l=0$, 1. It is known that a good fit to the $\pi\alpha$ data requires inclusion of the d wave. However, going to the next higher order in the expansion of M includes an su dependence as well as a t^2 dependence, and this rasies the question of s-channel poles. Naively expanding M to fourth order in the momenta, setting $p_2^2=p_4^2=m_\alpha^2$, and imposing crossing symmetry gives

$$M=a+bt+c(p_1^2+p_3^2)+dt^2+esu+ft(p_1^2+p_3^2)$$
$$+g(p_1^2+p_3^2)^2+hp_1^2p_3^2 \tag{76}$$

$$\xrightarrow[p_1\to 0]{} a+em_\alpha^4+(b+c)p_3^2+(d+f+g)p_3^4. \tag{77}$$

Using the condition that $\lim_{p_1\to 0} M\propto m_\pi^2-p_3^2$, we find that

$$a+em_\alpha^4=-m_\pi^2(b+c) \quad \text{and} \quad d+f+g=0.$$

On the mass shell, this gives an amplitude of the form

$$M(\text{on shell})=\text{const}+(b+2m_\pi^2 f)t+dt^2+esu. \tag{78}$$

Although at fixed s (for any T^{lab} in the region of interest 24–75 MeV) this formula gives a fairly good fit to the t dependence for $30°\lesssim\theta_{\text{c.m.}}\lesssim 150°$, it cannot be expected to represent the su dependence very well. The reason for this is the relative closeness of s- and u-channel singularities to the region of interest, in contrast to t-channel singularities.

The lowest t-channel singularity is the 2π branch point at $t=4m_\pi^2$, so a power expansion is good if $|t|<4m_\pi^2$, converging faster for smaller $|t|$. In the region of interest $-2m_\pi^2<t<0$.

No such favorable circumstances pertain to the s and u channels. Consider, for example, poles[33] at $m_{\alpha^*}\approx m_\alpha+25$ MeV (see Fig. 7) which contribute

$$\frac{1}{s-m_{\alpha^*}^2}+\frac{1}{u-m_{\alpha^*}^2}=\frac{2(m_\alpha^2+m_\pi^2-m_{\alpha^*}^2)-t}{su-[2(m_\alpha^2+m_\pi^2)-t]m_{\alpha^*}^2+m_{\alpha^*}^4}$$
$$\approx-\frac{2m_\pi^2-t}{m_\alpha^4}\left(1-\frac{su}{m_\alpha^4}\right)^{-1}. \tag{79}$$

This is approximately proportional to $1+su/m_\alpha^4$ only if $|su|\ll m_\alpha^4$. However, in the region of interest $|su|$ is of the order of m_α^4 or larger.

Thus, the s dependence of M in the region of interest cannot be represented satisfactorily by a power expansion in the momenta. For M(on shell) this can be handled simply by writing

$$M(\text{on shell})=a_s+b_st+c_st^2 \tag{80}$$

and experimentally determining a_s, b_s, and c_s for each value of s. However, there is no such easy way out for

[33] The α particle is a scalar isosinglet ^{4}He(3728.5). The two lowest sets of poles in the $\pi^\pm\alpha$ system are the isotriplets [^{4}H(3752.5), ^{4}He(3752.8), ^{4}Li(3753.0)] and [^{4}H(?), ^{4}He(3753.1 or 3755.0), ^{4}Li(3753.7 or 3756.2)], with $J^P=2^-$ and 0^-, respectively: W. E. Meyerhof and T. A. Tombrello, Nucl. Phys. **A109**, 1 (1968).

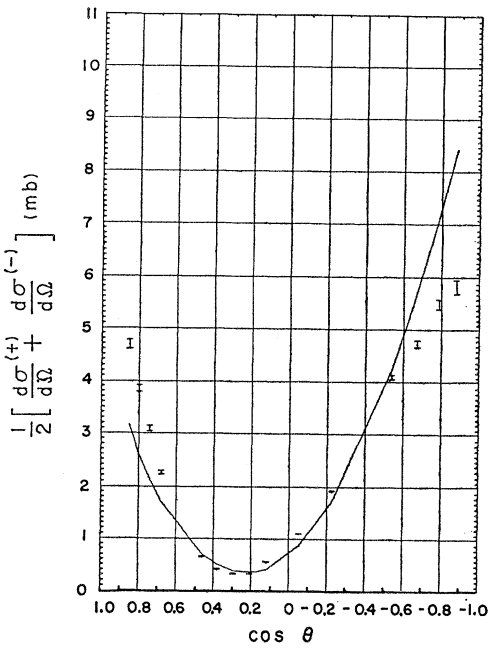

FIG. 8. Second-order expansion fitted to 60-MeV average cross section.

the fourth-order expansion of M(off shell). For the present we will have to live with the inherently less accurate

$$M(\text{off shell})=2B_s p_1\cdot p_3+C_s(t-m_\pi^2), \tag{74}$$

where the constants B_s and C_s are determined for each s by fitting $M(\text{on shell})=-(C_s-2B_s)m_\pi^2+(C_s-B_s)t$. The amount of inaccuracy in a second-order expansion relative to a fourth-order one can be observed by comparing the average cross-section fit of Fig. 8 (second order with $\chi_{\text{av}}^2=3033$) with that of Fig. 9(f) (fourth order with $\chi_{\text{av}}^2=68$).

IV. NUMERICAL RESULTS

A. Fitting Nuclear Parameters

Three sets of experimental $\pi^\pm\alpha$ scattering data are available (see Appendix B): (a) Rochester,[3] eight points at 24.0 MeV (1 s.d. errors $\approx 10\%$ in av cross sections); (b) Northwestern,[4] nine points each at 50, 58, and 65 MeV (1 s.d. errors $\approx 20\%$ in av cross sections); and (c) Berkeley,[5] 15 points each at 51.3, 59.7, 67.6, and 75.0 MeV (1 s.d. errors $\approx 3\%$ in av cross sections).

A least-squares search for values of the complex parameters a_s, b_s, and c_s which minimize

$$\chi_{\text{av}}^2=\sum_{i=1}^{N}\left[\frac{0.5(d\sigma^{(-)}/d\Omega_i+d\sigma^{(+)}/d\Omega_i)_{\text{expt}}-0.5(d\sigma^{(-)}/d\Omega_i+d\sigma^{(+)}/d\Omega_i)_{\text{calc}}}{(\text{expt error in average})_i}\right]^2 \tag{81}$$

was performed at each energy by using the fourth-order approximation to the on-shell strong amplitude

$$A_{\text{ST}}=a_s+b_s t+c_s t^2, \tag{82}$$

where the calculated average cross section is given by

$$0.5\left(\frac{d\sigma^{(-)}}{d\Omega}+\frac{d\sigma^{(+)}}{d\Omega}\right)_{\text{calc}}\approx\text{diagram in Fig. 10}$$

$$\approx(4/s)[|A_{\text{ST}}|^2+2\alpha\,\text{Re}A_{\text{ST}}^*(C_{\pi\pi}+D_\pi)+\alpha^2|A_{\text{C,B}}|^2]. \tag{83}$$

Using the fact that the $C_{\pi\pi}$ and D_π terms are small relative to A_{ST}, we omitted them in our initial determination of the strong-amplitude parameters.[34] Since the average cross section in this approximation is independent of the over-all phase of A_{ST}, there were five parameters to determine. The results are shown in Table IV and displayed in Fig. 9.

It was also necessary to perform a similar least-squares search using the less accurate expansion

$$A_{\text{ST}}=(1/16\pi)[(C_s-2B_s)m_\pi^2-(C_s-B_s)t] \tag{84}$$

in order to determine values for the second-order approximation to the off-shell amplitude. These results are given in Table V. (See Fig. 7 for a plot of the 60-MeV curve.)

B. Pion Form Factor

We now adjust the remaining parameters—r_π and the over-all phase of A_{ST}—to minimize

$$\chi_{\text{diff}}^2=\sum_{i=1}^{N}\left[\frac{(d\sigma^{(-)}/d\Omega_i-d\sigma^{(+)}/d\Omega_i)_{\text{expt}}-(d\sigma^{(-)}/d\Omega_i-d\sigma^{(+)}/d\Omega_i)_{\text{calc}}}{(\text{expt in error diff})_i}\right]^2, \tag{85}$$

[34] Furthermore, since $A_{\text{C,B}}$ is very small compared with A_{ST}, the exact value of r_π used for the average cross-section fit is unimportant. So we used $r_\pi=0.63$ F. For this same reason, the cross-section average fit was not used to determine the phase of A_{ST} relative to $A_{\text{C,B}}$.

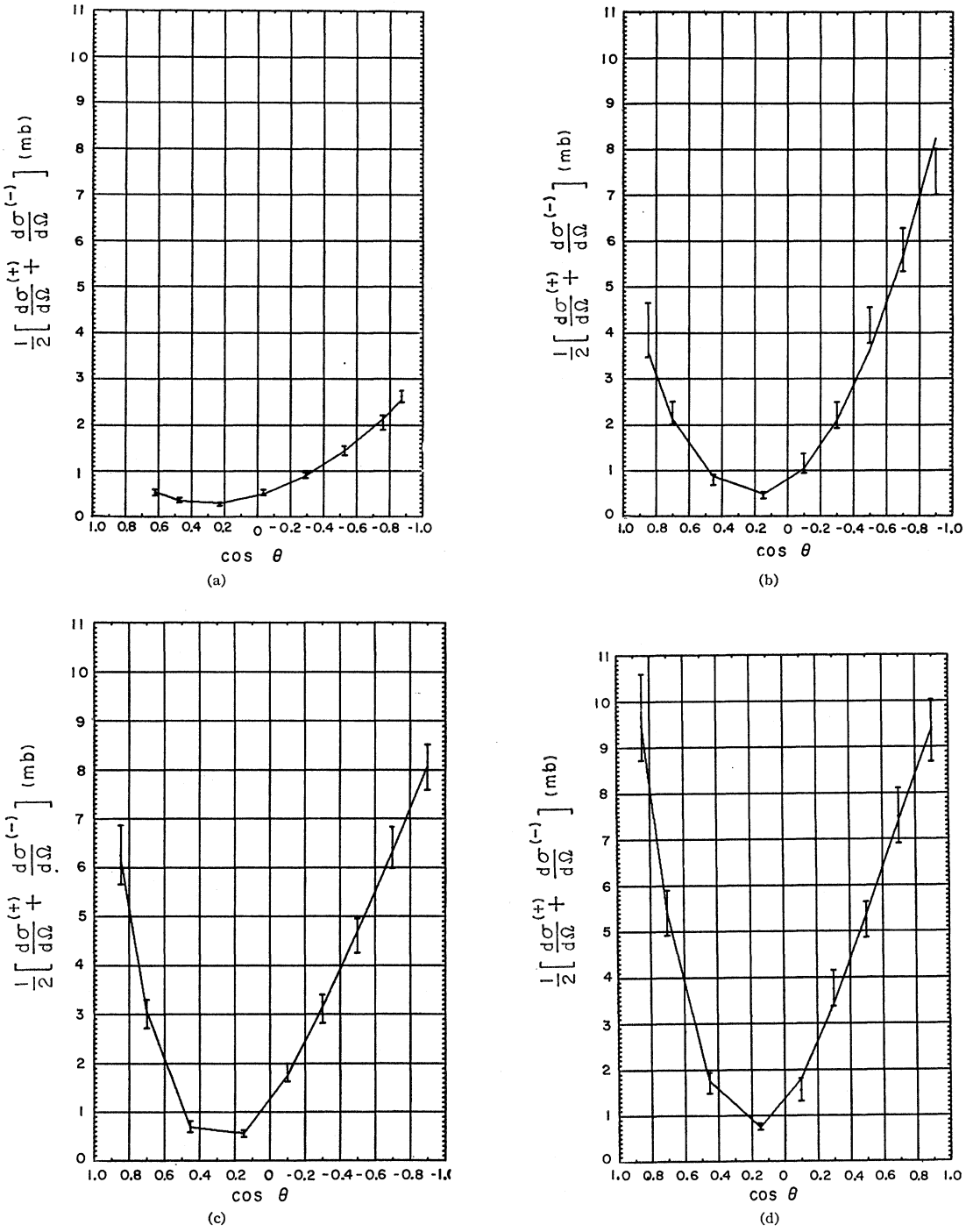

FIG. 9. Average cross section: (a) 24, (b) 50, (c) 58, (d) 65, (e) 51, (f) 60, (g) 68, (h) 75 MeV.

where the leading terms in the calculated cross-section difference are

$$\frac{d\sigma^{(-)}}{d\Omega}-\frac{d\sigma^{(+)}}{d\Omega}\approx\text{diagram in Fig. 11}$$
$$\approx-(4/s)\alpha\,\mathrm{Re}A_{\mathrm{ST}}{}^{*}[A_{\mathrm{C,B}}+C_{\pi\alpha}+D_{\alpha}]. \tag{86}$$

(We have dropped the z_π in $D_{\pi\alpha}$ and D_α.)

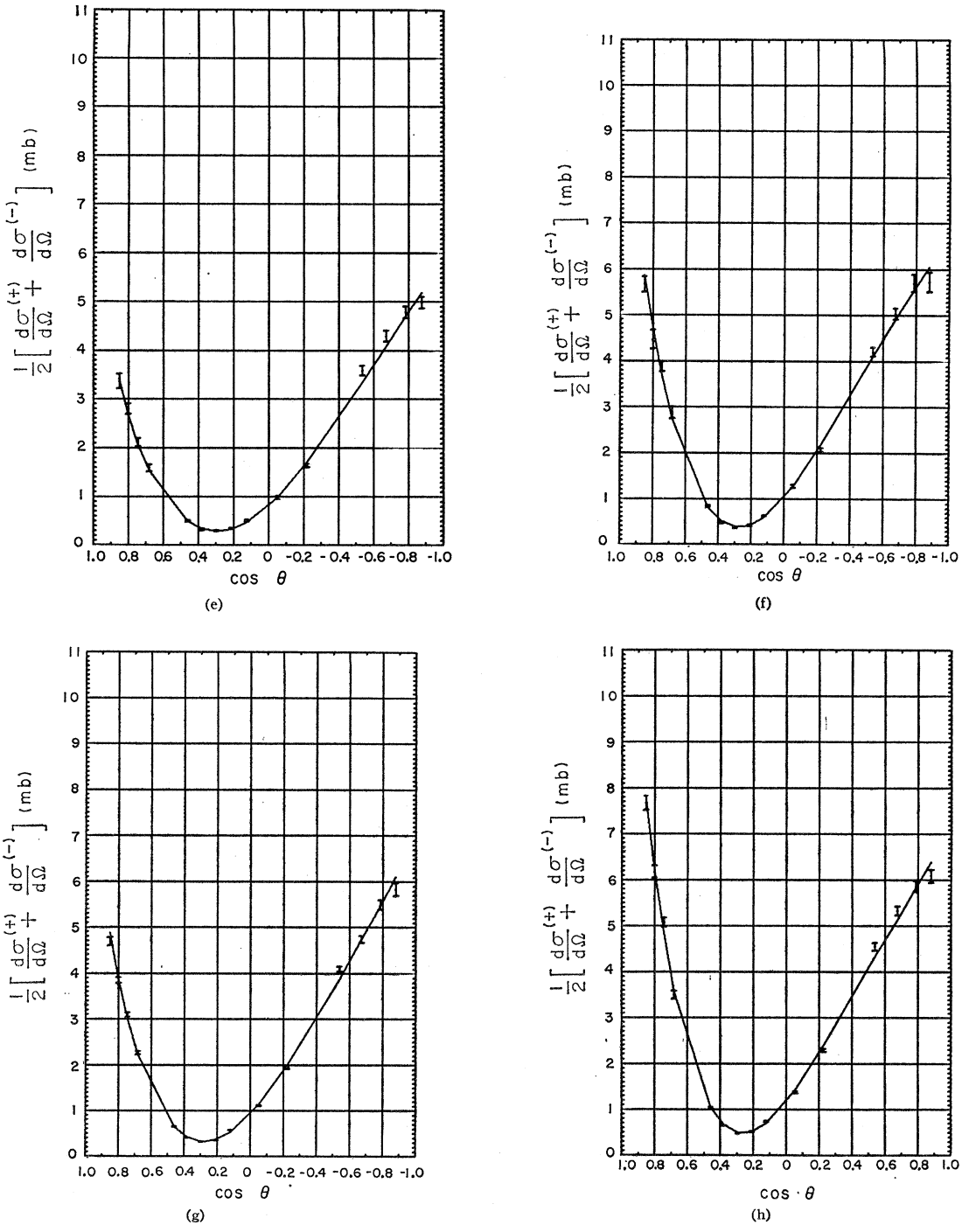

FIG. 9 (cont.).

The term D_α is calculated in Sec. II D:

$$D_\alpha=(0.056/16\pi^3)B_s(s-u)\,. \tag{87}$$

The term $C_{\pi\alpha}$ is given in Sec. II C:

$$C_{\pi\alpha}=2[C_{21}+C_{21}(p_2\leftrightarrow -p_4)], \tag{88}$$

TABLE IV. On-shell fourth-order nuclear parameters for Eq. (82).

T^{lab} (MeV)	a_s	b_s (10^{-4} MeV^{-2})	c_s (10^{-9} MeV^{-4})	χ_{av}^2	χ_{av}^2 (expected)
Rochester					
24.0	$-2.498-0.963i$	$-0.020-0.010i$	0	1.5	2
Northwestern					
50	$-6.608-0.926i$	$-2.597+0.475i$	$-0.020-0.010i$	5.8	3
58	$-9.959-0.413i$	$-4.708+0.212i$	$-3.723-1.248i$	0.3	3
65	$-11.975-0.890i$	$-4.228+0.457i$	$-2.138-0.194i$	1.9	3
Berkeley					
51.3	$-6.837-0.917i$	$-3.567+0.471i$	$-2.027+0.659i$	26	9
59.7	$-8.649-0.450i$	$-3.865+0.231i$	$-2.842-0.912i$	68	9
67.6	$-9.648-0.538i$	$-3.706+0.276i$	$-2.329-0.496i$	27	9
75.0	$-11.270-0.495i$	$-3.933+0.254i$	$-2.557-0.534i$	44	9

FIG. 10. Principal contributions to average cross section.

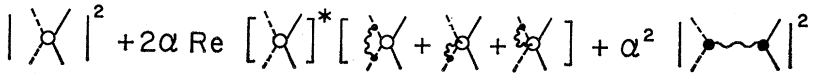

FIG. 11. Principal contributions to cross-section difference.

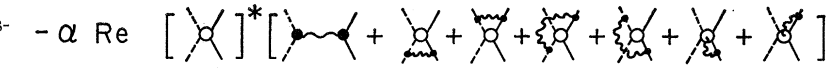

where, dropping the C_sq^4 contribution,[23] we get

$$C_{21}\approx-\frac{M_\alpha^2}{32\pi^2}\int_0^1 dx\int_0^x dy\left\{[4(p_1\cdot p_2)(g\cdot P)+(g\cdot P)(g\cdot Q)]\left[\frac{1}{M_\alpha^2}\left(\frac{1}{g^2}-\frac{1}{g^2-yM_\alpha^2}\right)\right.\right.$$
$$\left.+\frac{1}{M_\pi^2-M_\alpha^2}\left(\frac{1}{g^2-yM_\pi^2}-\frac{1}{g^2-yM_\alpha^2}\right)\right]+\frac{M_\pi^2}{M_\alpha^2-M_\pi^2}[4C_s(p_1\cdot p_2)+g\cdot(C_sQ-P)]\left.\left(\frac{1}{g^2-yM_\pi^2}-\frac{1}{g^2-yM_\alpha^2}\right)\right\}. \quad (89)$$

The y integration can be done analytically. We define

$$M_0^2\equiv 0, \quad (90)$$

$$-\Delta_i\equiv 4(1-x)^2[(p_1\cdot p_2)^2-m_1^2m_2^2]+M_i^4-4M_i^2p_1\cdot p_2(1-x)+8M_i^2xm_2^2, \quad (91)$$

where $i=0$, π, or α. Then the relevant integrals are

$$I_i(x)\equiv\int_0^x dy\,\frac{1}{g^2-yM_i^2}=\int_0^x\frac{dy}{a+by+cy^2}, \quad (92)$$

$$J_i(x)\equiv\int_0^x dy\,\frac{y}{g^2-yM_i^2}=\frac{1}{2c}\ln\left|\frac{a+bx+cx^2}{a}\right|-\frac{b}{2c}I_i(x), \quad (93)$$

$$K_i(x)\equiv\int_0^x dy\,\frac{y^2}{g^2-yM_i^2}=\frac{x}{c}-\frac{b}{2c^2}\ln\left|\frac{a+bx+cx^2}{a}\right|+\frac{b^2-2ac}{2c^2}I_i(x), \quad (94)$$

where

$$a\equiv m_1^2(1-x)^2-2p_1\cdot p_2x(1-x)+m_2^2x^2, \quad (95)$$

$$b\equiv 2p_1\cdot p_2(1-x)-2m_2^2x-M_i^2, \quad (96)$$

$$c\equiv m_2^2, \quad (97)$$

so that

$$-\Delta=b^2-4ac. \quad (98)$$

TABLE V. Off-shell second-order nuclear parameters for Eq. (84).

T^{lab} (MeV)	B_s (MeV^{-2})	C_s (MeV^{-2})		χ_{av}^2	χ_{av}^2 (expected)
Rochester					
24.0	0.0204	0.0344	$-0.00248i$	2	4
Northwestern					
50	0.0300	0.0430	$-0.00238i$	6	5
58	0.0296	0.0412	$-0.00247i$	52	5
65	0.0370	0.0494	$-0.00247i$	38	5
Berkeley					
51.3	0.0240	0.0346	$-0.00212i$	471	11
59.7	0.0272	0.0381	$-0.00192i$	3033	11
67.6	0.0266	0.0361	$-0.00192i$	1075	11
75.0	0.0276	0.0364	$-0.00192i$	3159	11

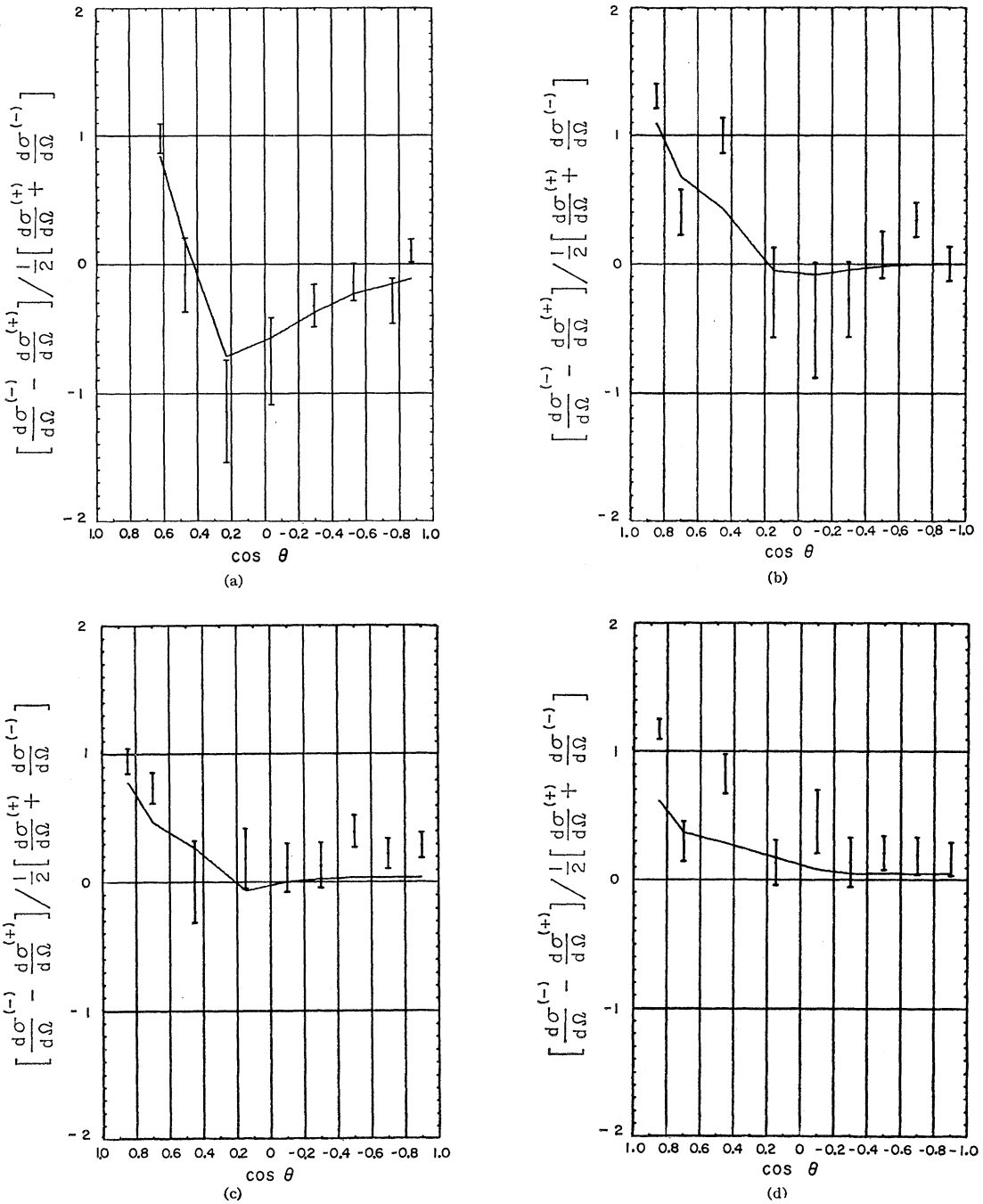

FIG. 12. Ratio of cross-section difference to average cross section: (a) 24, (b) 50, (c) 58, (d) 65, (e) 51, (f) 60, (g) 68, (h) 75 MeV

Doing the x integration in $C_{\pi\alpha}$ numerically and fitting to the cross-section difference data, we obtain the results shown in Table VI and displayed in Fig. 12. The over-all phases θ_4 and θ_2 are those associated with the fourth- and second-order expansions of A_{ST}.

The reasonableness of the phases θ_4 obtained can be checked against data on the total cross section (inelastic as well as elastic) by use of the optical theorem[35]

$$\mathrm{Im}A_{ST}(t=0)=-\frac{2k\sqrt{s}}{16\pi}\sigma_{\mathrm{tot}}{}^{\mathrm{nucl}}. \tag{99}$$

The measured total nuclear cross sections at 50, 58,

[35] The author is grateful to Professor A. Wolfenstein for suggesting this cross-check.

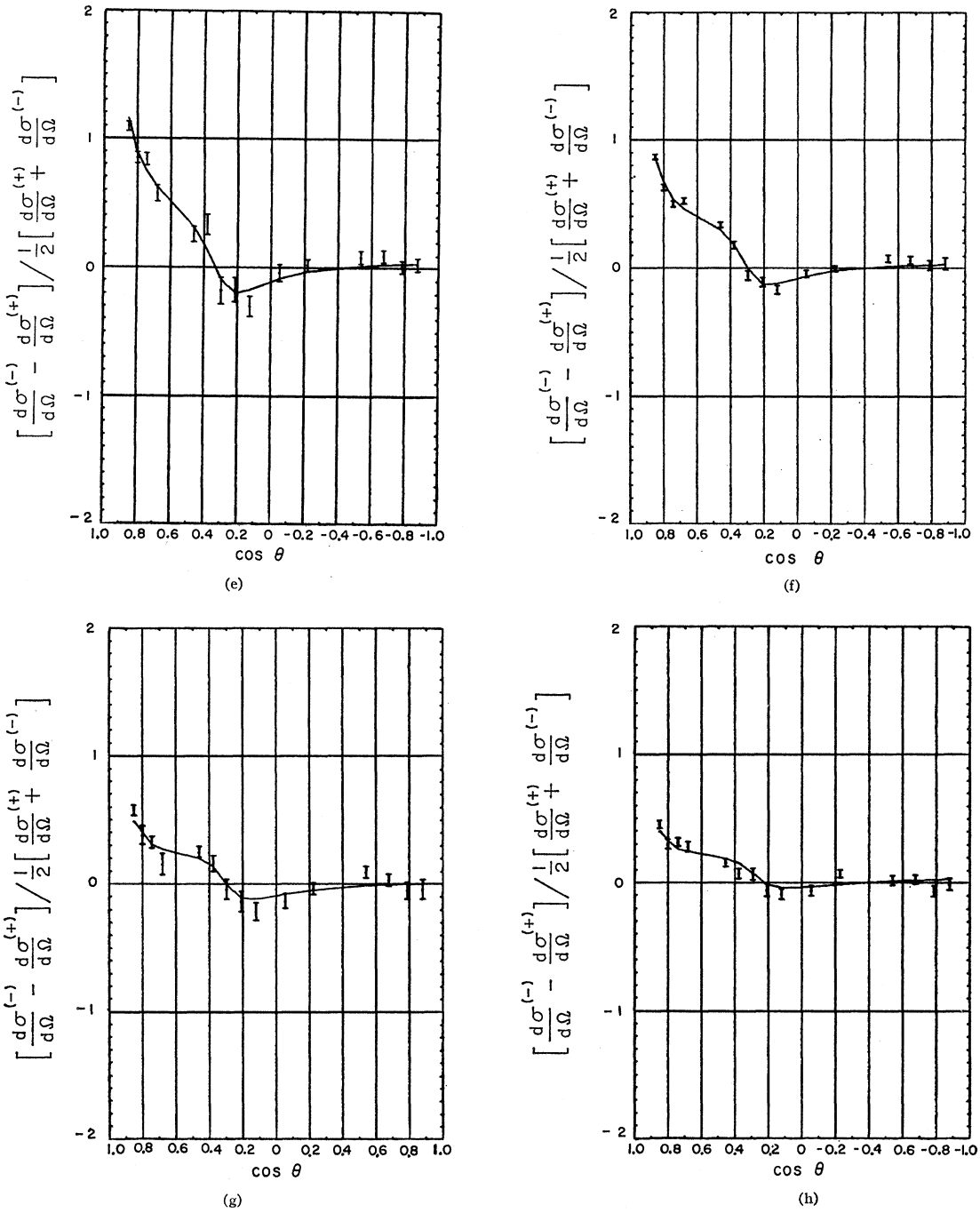

FIG. 12 (cont.).

and 65 MeV are quoted[4] as 87.6±3.0, 98.2±2.7, and 123.2±3.7 mb, respectively. The total cross sections implied by the phases in Table VI for the Northwestern data are much smaller than the measured values (59 mb for the 58-MeV phase). However, the Berkeley data, which have smaller experimental errors and present less problems regarding nearly equivalent local minima to the χ^2-minimizing search program used to obtain θ_4, give 54, 81, 127, and 137 mb (with uncertainty about ±20%, not counting effects of theoretical approximations in the distortion term) as the total cross sections implied by the phases at 51, 60, 68, and 75 MeV.

TABLE VI. Pion charge radius, taking the cross-section difference proportional to $\mathrm{Re}A_{ST}^{*}(A_{C,B}+C_{\pi\alpha}+D_{\alpha})$, where $C_{\pi\alpha}$ is computed using an off-shell strong amplitude accurate only to second order in the momenta and D_{α} is computed assuming soft-photon dominance of the integral over virtual photon momenta. The values of χ^2 are not intended to reflect these theoretical uncertainties, which could have a strong effect on r_{π}.

T^{lab} (MeV)	r_{π} (F)	θ_4 (rad)	θ_2 (rad)	χ_{diff}^2	χ_{diff}^2 (expected)
Rochester					
24.0	0.87	0.287	−0.483	11	4
Northwestern					
50	1.46	−0.137	−0.407	13	5
58	1.31	0.297	−0.615	16	5
65	1.00	0.198	−1.437	17	5
Berkeley					
51.3	0.85	0.287	−0.483	16	11
59.7	0.66	0.513	−0.757	21	11
67.6	0.99	0.890	−1.502	15	11
75.0	0.99	0.889	−1.502	25	11

1. *Sensitivity of r_{π} to Relativistic Terms*

All of the previous computations[3–9,36] of the pion charge radius based on $\pi\alpha$ scattering measurements have used nonrelativistic dynamics, i.e., they involved inserting interaction potentials into either the Schrödinger or the Klein-Gordon wave equation. The use of a wave equation automatically considers the electromagnetic interaction represented by the potentials to all orders. Use of the Klein-Gordon equation provides relativistically correct kinematics. The use of wave-equation-constrained wave functions properly fitted to the data assures reasonable off-shell behavior. However, use of a dynamically nonrelativistic wave equation (as distinguished from the Bethe-Salpeter equation, for example) ingores all diagrams in which the interactions represented by the potentials do not occur in a definite time sequence. For example, it ignores the diagrams shown in Figs. 2(b) and 2(c), in which the electromagnetic and nuclear interactions overlap the same time interval, and those shown in Figs. 3(c) and 3(d), in which the electromagnetic interaction overlaps part of the nuclear interaction.

TABLE VII. Comparison of relativistic and nonrelativistic calculations of r_{π}.

	Relativistic (from Table VI)		Nonrelativistic			
T^{lab} (MeV)	r_{π} (F)	χ_{diff}^2	r_{π} (F)	θ_4 (rad)	θ_2 (rad)	χ_{diff}^2
Rochester						
24.0	0.87	11	1.46	0.115	−2.824	8
Northwestern						
50	1.46	13	1.90	−0.013	−0.940	13
58	1.31	16	2.91	−0.023	−1.022	15
65	1.00	17	1.45	−0.476	1.042	18
Berkeley						
51.3	0.85	16	2.90	0.219	−0.299	21
59.7	0.66	21	2.45	0.420	−0.900	32
67.6	0.99	15	2.39	0.640	0.100	15
75.0	0.99	25	2.39	0.619	0.878	17

As we have seen, $C_{\pi\alpha}$ and D_{α} are the dominant distortion terms. $C_{\pi\alpha}$ is composed of $C_{12}+C_{34}$, which enters into nonrelativistic calculations, and also the relativistic contribution $C_{41}+C_{23}$. D_{α} does not enter at all into nonrelativistic calculations. In order to compare this analysis with previous nonrelativistic calculations, the r_{π} calculation was rerun with the relativistic terms omitted. Table VII compares these results to those obtained by using D_{α} and the full $C_{\pi\alpha}$.

Two features are of interest. First, compare the respective χ_{diff}^2's. If the nonrelativistic terms alone fit the data poorly, anyone performing a nonrelativistic calculation would be immediately led to suspect the importance of the relativistic terms. However, the nonrelativistic terms alone fit the cross-section difference data about as well as the fully relativistic formulation. Second, without the relativistic terms, the estimates of r_{π} are larger, falling in the vicinity of the values for the Berkeley data obtained by using the Kisslinger model with the methods of Auerbach *et al.* and Block (Table II), both nonrelativistic methods. (This, incidentally, provides some evidence that the off-shell behavior of the amplitude used in computing $C_{\pi\alpha}$ is probably not too unreasonable.) Thus, even though the data can be fitted fairly well by using only the nonrelativistic terms, the relativistic terms are quite important in determining the value of r_{π}.

2. *Sensitivity of r_{π} to Nuclear Model*

It is clear that the value of r_{π} obtained through the type of analysis performed here is dependent upon the functional form assumed for the strong $\pi\alpha$ scattering amplitude. This is because the estimate of r_{π} is sensitive to the nuclear distortion, $C_{\pi\alpha}$ and D_{α} are the dominant parts of the distortion, and both of them depend in detail upon the form of the off-shell strong amplitude.

In order to get a numerical estimate of the model-dependent uncertainty in r_{π} it would appear to be necessary to recalculate $C_{\pi\alpha}$ and D_{α} by using a variety of off-shell models. However, we can get a rough idea of this uncertainty without doing such a set of complete recalculations.

First, we can simply increase or decrease $C_{\pi\alpha}$ or D_{α} by a factor roughly indicative of the error in the second-order amplitude given by Eq. (84). Looking at Fig. 8, which shows the average cross section (proportional to the absolute square of the amplitude), we see that on the mass shell this error is in the order of 10% (what it is off the mass shell is unknown). The calculation described in Sec. IV B was rerun varying $C_{\pi\alpha}$ and D_{α} by 10% in Eq. (86). The resulting shifts in r_{π} were

[36] C. T. Mottershead, University of California Lawrence Radiation Laboratory Report No. UCRL-19216, 1969 (unpublished). This is the most recent nonrelativistic analysis of the $\pi\alpha$ data, and discusses in detail the relative insensitivity of the results to the model-dependent shape of the nuclear radial wave function.

less than 1% (principally because of $A_{C,B}$), and the increases in χ_{diff}^2 were less than 1. (If $C_{\pi\alpha}$ is multiplied by 0.5 and D_α by zero, which is effectively what is done when only the nonrelativistic terms are considered, the shift in r_π for this local minimum in χ_{diff}^2 is still small. What happens is that the χ_{diff}^2 for this local minimum increases and that for a local minimum at larger r_π decreases, resulting in the larger r_π having lower χ_{diff}^2.)

Second, we can vary the on-shell amplitude A_{ST} in Eq. (86), leaving fixed the off-shell form used in calculating $C_{\pi\alpha}$ and D_α. This can be expected to have a more marked effect on r_π, since the expression in Eq. (86) is wholly proportional to A_{ST}. However, we do not have as much leeway in varying the on-shell amplitudes, since the $l=0$, 1, 2 expansion (82) fits the data so well.

Three approaches were tried. First, it was observed that the average deviations between model and experiment for A_{ST} using the parameters given in Table IV are: 24 MeV—1.9%, 50 MeV—3.9%, 58 MeV—0.8%, 65 MeV—2.0%, 51 MeV—1.9%, 60 MeV—1.3%, 68 MeV—1.9%, and 75 MeV—1.4%. (These are half the percentage deviations in the cross-section average which is proportional to the square of A_{ST}.) Varying A_{ST} by these amounts in Eq. (86) produced variations of about 1% in r_π.

Next, an $l=3$ term $d_s l^3$ was added to Eq. (82) and the whole calculation was rerun for the 60-MeV data, since these quite precise data afforded the best chance of detecting any $l=3$ contribution. The best fit was obtained for $d_s=0$, producing no shift in r_π.

Finally, A_{ST} was multiplied by a real θ-dependent phase $\psi(\theta)$:

$$A_{ST}(\text{new})=A_{ST}(\text{old})e^{i\psi(\theta)}. \tag{100}$$

Clearly this cannot affect χ_{av}^2 (neglecting the small correction term $2\alpha\,\mathrm{Re}A_{ST}{}^*C_{\pi\pi}$). Then $\psi(\theta)$ was set

$$\psi(\theta)=\epsilon\theta \tag{101}$$

and χ_{diff}^2(new) was computed as a function of ϵ, looking for the range of r_π for which $\chi_{diff}^2(\text{new})\leq\chi_{diff}^2(\text{old})$. Depending upon the energy, this range covered $\pm 50\%$ of r_π(old). However, this represents a rather artificial situation in which many higher partial waves enter in such a way as to cancel out in the cross-section average calculations, but strongly affect the cross-section difference results. It appears to be more physically reasonable to accept the conclusion that $l=3$ and higher waves are neglibible.

V. SUMMARY AND CONCLUSIONS

A relativistically complete examination has been made of all first-order electromagnetic corrections to $\pi^\pm\alpha$ scattering, by use of a low-momentum-transfer approximation to the off-shell strong amplitude.

For purposes of determining r_π, those corrections are most important which contribute to the difference between the $\pi^+\alpha$ and the $\pi^-\alpha$ cross sections. The Born Coulomb term, of course, dominates near the forward direction. All real infrared photon terms were found to be negligible in the relevant experiments. Of the remaining corrections, the ones which contribute significantly to the cross-section difference are those in which a virtual photon links an external α leg either to an external pion or to an internal line. Soft-photon dominance was assumed in showing that if one end of the virtual photon terminates inside the strong interaction, then if the other end also terminates internally, the term is negligible, whereas if the other end terminates on an external pion, the term contributes to the cross-section average rather than to the difference.

In spite of the fact that a fairly good fit to the cross-section difference data can be obtained by using only the diagrams in which a virtual photon links either both incoming particles or both outgoing particles, the purely relativistic diagrams were found to be equally important. Furthermore, when the relativistic terms were included, the best fits were obtained for significantly lower values of r_π.

Four amplitudes (A_{ST},$A_{C,B}$,$C_{\pi\alpha}$, and D_α) were computed in the process of extracting an estimate of r_π from cross-section difference data. The forms taken for the on-shell strong amplitude A_{ST} and the Born Coulomb amplitude $A_{C,B}$ are sufficiently accurate for this purpose when using the most precise of the available data. The possible sources of error are the estimated form of $C_{\pi\alpha}$ (the amplitude for a photon linking an external pion to an external α particle), the estimated form of D_α (the amplitude for a photon linking an external α particle to an internal line), and the estimated negligibility of the contributions of D_π and D_0 to the cross-section difference. The form taken for $C_{\pi\alpha}$ uses an off-shell strong amplitude accurate only to second order in the momenta, and that taken for D_α assumes soft-photon dominance of the integral in Eq. (49). (The justification for neglecting D_π and D_0 also assumes soft-photon dominance.)

Using these forms, $C_{\pi\alpha}$ and D_α are of roughly the same magnitude. In the forward direction $A_{C,B}$ dominates over them. In the region from roughly 60° to 180°, $C_{\pi\alpha}$ and D_α contribute more to the cross-section difference than $A_{C,B}$. Both the $C_{\pi\alpha}$ and the D_α contributions in this region differ in sign from that of $A_{C,B}$, resulting in a fit to the data at smaller r_π. (Furthermore, all four components of $C_{\pi\alpha}$ contribute with the same sign, so if C_{14}, C_{23}, and D_α are omitted, the apparent value of r_π is increased.)

However, before a definitive value for r_π based on $\pi^\pm\alpha$ scattering can be quoted it will be necessary to clear up the following three problems.

(a) The theoretical problem of calculating the hard-photon parts of virtual internal terminating corrections. This is the difficult and important problem of extending the low-energy bremsstrahlung theorem to say something about $O(q)$ terms in the $ab\to ab\gamma$ amplitude.

These terms may turn out to be negligible for purposes of determining r_π, but there is as yet no way of knowing whether or not this is the case.

(b) The theoretical problem of finding an off-shell model of the amplitude valid at least up to terms of order t^2, i.e., fourth order in momentum. That the second-order approximation used here is sufficiently inaccurate to affect the determination can be seen by comparing the on-shell second- and fourth-order approximations.

(c) The experimental problem of reducing the erorrs enough to see at least the $l=3$ waves in the cross-section average. Information concerning higher waves is necessary because the r_π determination, which uses the cross-section difference, is fairly sensitive to the detailed structure of the functional form used for the strong amplitude.

ACKNOWLEDGMENTS

The author thanks Joel Yellin for suggesting this problem and providing guidance, and Korkut Bardakci, Geoffrey Chew, Kenneth Crowe, Anthony Fainberg, Stanley Mandelstam, Thomas Mottershead, Arnulf Rabl, and Al Wolfenstein for helpful discussions and comments.

APPENDIX A: NONRELATIVISTIC STERNHEIM-HOFSTADTER PROGRAM

In this appendix we give a brief review of the Sternheim-Hofstadter (SH)[1] program for measuring the pion electromagnetic form factor as formulated by Schiff,[2] together with a summary of three techniques used for adapting this formulation to analysis of experimental data.

Schiff's nonrelativistic formalism begins with Goldberger and Watson's[37] expression for the T-matrix element for scattering by the sum of two potentials $U=2\mu u$ and $V=2\mu v$ $[\mu=m_\pi m_\alpha/(m_\pi+m_\alpha)]$,

$$T_{fi}=(\phi_f^-,U\chi_i)+(\phi_f^-,V\psi_i^+), \tag{A1}$$

where[38]

$$(\nabla^2+k^2)\chi=0, \tag{A2}$$

$$(\nabla^2+k^2-U)\phi=0, \tag{A3}$$

$$(\nabla^2+k^2-U-V)\psi=0. \tag{A4}$$

V is taken to be the Born Coulomb potential, shown to first order for $\pi\alpha\rightarrow\pi\alpha$ in Fig. 1. [Thus, in coordinate space to first order, v is the Fourier transform of $F_\pi(q^2)F_\alpha(q^2)/q^2$.] U then represents the total potential minus V. In the absence of electromagnetic effects, U is simply the strong potential. More specifically $U=U_s-(V-V_0)$, where U_s is the purely strong potential and V_0 is the point Coulomb potential.

[37] M. L. Goldberger and K. M. Watson, *Collision Theory* (John Wiley & Sons, Inc., New York, 1964), p. 203.

[38] Superscripts + and − indicate outgoing and incoming plane waves, respectively. The χ represents the initial plane-wave state.

The expectation is that U_s will be the same for $\pi^+\alpha$ and $\pi^-\alpha$ scattering, and the V's will differ only in sign. To first order in the electromagnetic interactions, we have

$$d\sigma^{(\pm)}/d\Omega\propto|(\phi_f^-,U^\pm\chi_i)|^2 +2\,\mathrm{Re}[(\phi_f^-,U^\pm\chi_i)^*(\phi_f^-,V^\pm\psi_i^+)]. \tag{A5}$$

Then, using the assumption $U_s^+=U_s^-$, $V^+=-V^-$, we have

$$\frac{1}{2}\left[\frac{d\sigma^{(+)}}{d\Omega}+\frac{d\sigma^{(-)}}{d\Omega}\right]\propto|(\phi_f^-,U_s\chi_i)|^2, \tag{A6}$$

$$\frac{1}{2}\left[\frac{d\sigma^{(+)}}{d\Omega}-\frac{d\sigma^{(-)}}{d\Omega}\right]\propto 2\,\mathrm{Re}[(\phi_f^-,U\chi_i)^*(\phi_f^-,V^+\psi_i^+)]. \tag{A7}$$

The SH program then is this: Choose a model for the strong interactions which gives U as a function of certain parameters. Using experimental data on the cross-section average, determine values of these parameters which give a good fit to the data. These values, which determine $(\phi_f^-,U_s\chi_i)$, can then be used together with cross-section difference data to ascertain parameters such as r_π in the first-order expression for $(\phi_f^-,V\psi_i^+)$, since the term $(\phi_f^-,(V-V_0)\chi_i)$ contributes only in second order.

To formulate the SH program even more explicitly, Schiff assumed U to be spherically symmetric and let

$$\phi(\mathbf{x})=\sum_{l,m} rR_l(r)Y_l^m(\theta,\phi), \tag{A8}$$

where $R_l(r)$ is the lth partial nuclear radial wave function. Then

$$f_N(\theta)=-\frac{1}{4\pi}(\phi_f^-,U\chi_0)=\frac{1}{k}\sum_{l=0}^{\infty}(2l+1)\frac{e^{2i\delta_l}-1}{2i}P_l(\cos\theta), \tag{A9}$$

where the δ_l are the hadronic phase shifts, which are in general complex.

Schiff showed that to first order one can substitute ϕ_i^+ for ψ_i^+ in the expression $(\phi_f^-,V\psi_i^+)$ and obtain (defining $q=2k\sin\frac{1}{2}\theta$)

$$(\phi_f^-,V\phi_i^+)=4\pi\int_0^\infty V(r)j_0(qr)dr+4\pi\sum_{l=0}^{\infty}(2l+1)P_l(\cos\theta) \times\int_0^\infty V(r)[e^{2i\delta_l}R_l^2(r)-j_l^2(kr)]r^2dr, \tag{A10}$$

a form in which the Born amplitude is explicitly separated out. The amplitude $f_V=-(1/4\pi)(\phi_f^-,V\psi_i^+)$ can thus be written as the sum of the Born amplitude and the Schiff distortion amplitude:

$$f_V=f_{C,B}+f_{CN}. \tag{A11}$$

The distortion amplitude f_{CN} contains all nonrelativistic first-order electromagnetic effects not contained in the first-order Born Coulomb amplitude:

$$f_{C,B}=-\int_0^\infty V(r)j_0(qr)dr, \tag{A12}$$

$$f_{CN}=-\sum_{l=0}^{\infty}(2l+1)P_l(\cos\theta)\int_0^\infty V(r) \times[e^{2i\delta_l}R_l^2(r)-j_l^2(kr)]r^2dr. \tag{A13}$$

Because the Coulomb field is long-range, both integrals diverge at the upper limit, so a physically meaningful cutoff must be introduced such as the average separation between nuclei in the experimental medium, beyond which the field from the nucleus of interest is masked by the surrounding fields. This distance is ordinarily in the order of 10^{-8} cm.

As an alternative way of avoiding the divergences, West[6] uses a different separation based on pulling out the point Coulomb amplitude,

$$f_V=f_C+f_{\Delta V}+f_{CN}', \tag{A14}$$

where

$$f_C=-(2nk/q^2)e^{-in\ln\sin^2(\frac{1}{2}\theta)+2i\eta_0}, \qquad \eta_0=-0.5772n \tag{A15}$$

$$f_{\Delta V}=-\int_0^\infty[V(r)-V_0(r)]j_0(qr)r^2dr, \tag{A16}$$

$$f_{CN}'=-\sum_{l=0}^{\infty}(2l+1)P_l(\cos\theta)\int_0^\infty V(r) \times\left[e^{2i\delta_l}R_l^2(r)-j_l^2(kr)-\frac{e^{2i\delta_l}-1}{2k^2r^2}\right]r^2dr. \tag{A17}$$

Still another breakdown is used by Block,[8] who shows that to first order

$$f_V\approx f_B+f_D, \tag{A18}$$

where

$$f_B=f_{C,B}+\frac{1}{k}\sum_{l=0}^{\infty}(2l+1)P_l(\cos\theta)(e^{2i\delta_l}-1)(\eta_l-\eta_0) \tag{A19}$$

and

$$f_D=\frac{1}{k}\sum_{l=0}^{\infty}(2l+1)P_l(\cos\theta)e^{2i\delta_l}nx_l, \tag{A20}$$

with

$$nx_l=-k\int_0^\infty V(r)[R_l^2(r)-j_l^2(kr)]r^2dr. \tag{A21}$$

Auerbach *et al.*[9] used the original breakout

$$f^{(\pm)}=f_N\pm(f_{C,B}+f_{CN}) \tag{A22}$$

$$=\pm f_C+\frac{1}{k}\sum_{l=0}^{\infty}(2l+1)P_l(\cos\theta)[(f_N)_l\pm(f_{CN})_l \pm(f_{C,B}-f_C)_l], \tag{A23}$$

and obtain $(f_N)_l$ and $(f_{CN})_l$ from $f_l^{(\pm)}$ and $(f_{C,B})_l$ via

$$(f_N)_l=\tfrac{1}{2}[f_l^{(+)}+f_l^{(-)}], \tag{A24}$$

$$(f_{CN})_l=\tfrac{1}{2}[f_l^{(+)}-f_l^{(-)}-2(f_{C,B})_l]. \tag{A25}$$

In addition to using different techniques for overcoming the Coulomb potential divergences, these three approaches also used different models for the nuclear interaction.

To represent the data satisfactorily, a model of nuclear $\pi\alpha$ scattering must take absorption into consideration.[39] In addition, it is known from partial-wave analyses of other pion-nuclear interactions[40] that, unlike the cases of nucleons and α particles scattering on nuclei, which seem well approximated by local potentials, pion-nuclear interactions apparently cannot be explained unless nonlocality is employed.

Block[8] introduced a certain form of nonlocality into a purely phenomenological Gaussian potential by making it spin-dependent:

$$U_l(r)=U_l(0)e^{-3r^2/(r_\pi^2+r_\alpha^2)}, \tag{A26}$$

where the $U_l(0)$ were permitted to be complex to simulate absorption.

West[7] and Auerbach *et al.*[9] both used the Kisslingre model,[41] based on the impulse approximation that individual nucleons in the nucleus behave under impact like free nucleons which are, however, spread throughout the nucleus according to a nuclear density function $\rho(\mathbf{r})$. This yields a momentum-dependent potential

$$U^{\mathrm{Kis}}(r)=-(4\pi/2\mu)[b_0\rho(r)-\nabla\cdot c_0\rho(r)\nabla]. \tag{A27}$$

In both cases, the original Kisslinger model was modified by allowing b_0 and c_0 to be complex to simulate absorption.[42] If $\mathrm{Im}c_0=0$, the differential equation arising from the model contains a singularity. To avoid this, West further modified the model by making the replacement

$$(1+\rho_0 c)\rightarrow(1-\rho_0 c)^{-1}. \tag{A28}$$

[39] The total elastic and inelastic cross sections have been measured at 129, 140, and 150 MeV/c for both $\pi^+\alpha$ and $\pi^-\alpha$ scattering. In all cases $\sigma_{\mathrm{inel}}>\sigma_{\mathrm{el}}$. Compare with M. Block *et al.*, Phys. Rev. **169**, 1074 (1968). The observed absorption modes of low-energy $\pi^-\alpha$, for example, include *td*, *d2n*, and *p3n* in proportions 30:54:16%: M. Schiff, R. H. Hildebrand, and C. Giese, *ibid.* **122**, 265 (1961); S. G. Ekstein, *ibid.* **129**, 413 (1963). In addition, there are three- and five-body channels, the inelastic modes without charge exchange, $\pi^-n\mathrm{He}^3$, π^-2n2p, and $\pi^-p\mathrm{H}^3$, and those with charge exchange, $\pi^0n\mathrm{H}^3$ and π^0p3n. At 153 MeV, elastic scattering is 36% of the total, while the three-body modes without charge exchange are 20, 10, and 4%, respectively, leaving 30% for the sum of the three-body modes with charge exchange and the pion absorption modes: Y. A. Budagov *et al.*, Zh. Eksperim. i Teor. Fiz. **42**, 1911 (1961) [English transl.: Soviet Phys.—JETP **15**, 824 (1962)].

[40] W. F. Baker *et al.*, Phys. Rev. **112**, 1763 (1958); **112**, 1773 (1958); M. Ericson, Compt. Rend. **257**, 3831 (1963).

[41] L. Kisslinger, Phys. Rev. **98**, 761 (1955).

[42] Considering the more detailed results of M. Ericson and T. E. O. Ericson [Ann. Phys. (N. Y.) **36**, 323 (1966)], it may have been better to introduce complex parameters by writing $U(\mathbf{r})\approx-(4\pi/2\mu)\{[b_0+B_0\rho(\mathbf{r})]\rho(\mathbf{r})-\nabla\cdot[c_0+C_0\rho(\mathbf{r})]\rho(\mathbf{r})\nabla\}$, where b_0 and c_0 are real and B_0 and C_0 are complex.

West used a step-function density $\rho(\mathbf{r})=\theta(R)$. Auerbach *et al.* used two different nuclear density functions, the modified Gaussian of the shell model and the modified exponential of the Saxon-Woods model.

APPENDIX B: $\pi\alpha$ SCATTERING DATA

The basic $\pi^{\pm}\alpha$ scattering data from Refs. 3–5 are given in Tables VIII–X. The Northwestern and Berkeley data, which cover roughly the same energy range, appear to be inconsistent, even discounting the problem of uncertainty in over-all normalization (cited as ± 6 and $\pm 2\%$ for the Northwestern and Berkeley data, respectively). A plot of the data at constant values of the scattering angle is shown in Fig. 13. Although experimental errors are quite large, the Northwestern cross sections appear to increase consistently faster with s than those measured at Berkeley.

The Northwestern curves in Fig. 13 were drawn using the center of each $(\Delta\cos\theta,\Delta d\sigma/d\Omega)$ bin in the published data. Because of the forward and backward peaking, the event distribution in each bin was probably weighted toward the side with greater $|\cos\theta|$. Thus, if we use the center of the $\Delta d\sigma/d\Omega$ range of the bin as the cross section for the datum point, we should use a value of $\cos\theta$ between the center and the larger extreme.

If μ_L and μ_U are the extremum values of $\cos\theta$ for a

TABLE VIII. Rochester data (at 24 MeV).

$\theta_{c.m.}$ (deg)	$d\sigma^+/d\Omega$ (mb/sr)	ϵ_+ (mb/sr)	$d\sigma^-/d\Omega$ (mb/sr)	ϵ_- (mb/sr)
51.6	0.27	0.05	0.79	0.11
61.8	0.38	0.06	0.35	0.08
76.9	0.44	0.05	0.12	0.05
92.0	0.73	0.05	0.33	0.12
107.0	1.04	0.08	0.75	0.10
121.8	1.53	0.15	1.33	0.13
139.3	2.33	0.16	1.75	0.27
150.9	2.48	0.12	2.75	0.22

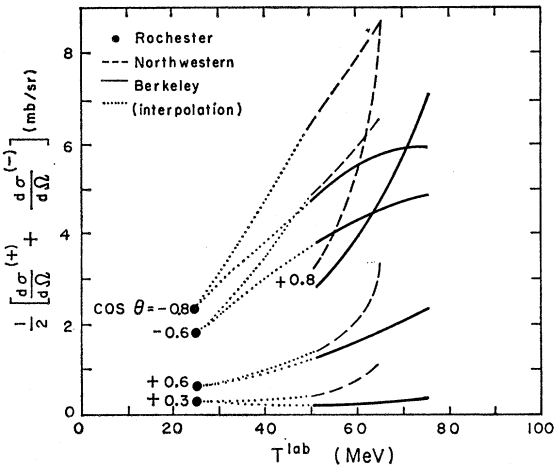

FIG. 13. Average cross sections at constant scattering angle.

TABLE IX. Northwestern data.

$\theta_{c.m.}$ (deg)	$d\sigma^+/d\Omega$ (mb/sr)	$(d\sigma^+/d\Omega)_{mod}$ (mb/sr)	ϵ_+ (mb/sr)	$d\sigma^-/d\Omega$ (mb/sr)	$(d\sigma^-/d\Omega)_{mod}$ (mb/sr)	ϵ_- (mb/sr)
			50 MeV			
31.8	1.6	1.4	0.4	7.0	6.7	1.1
45.6	1.8	1.8	0.3	2.8	2.7	0.4
63.2	0.4	0.4	0.1	1.3	1.2	0.2
81.4	0.5	0.5	0.1	0.4	0.4	0.1
95.7	1.5	1.4	0.3	1.1	0.9	0.3
107.5	2.6	2.5	0.4	2.1	1.9	0.4
120.0	4.1	4.0	0.5	4.4	4.3	0.6
134.4	4.9	4.8	0.5	7.0	6.8	0.8
154.2	7.6	7.5	0.6	7.7	7.5	0.8
			58 MeV			
31.8	3.4	3.3	0.5	9.4	9.2	1.1
45.6	2.0	1.9	0.3	4.2	4.1	0.5
63.2	0.7	0.7	0.1	0.8	0.7	0.2
81.4	0.5	0.5	0.1	0.6	0.6	0.1
95.7	1.7	1.7	0.2	2.0	1.9	0.3
107.5	3.0	2.9	0.3	3.4	3.3	0.5
120.0	3.8	3.7	0.4	5.6	5.5	0.6
134.4	5.8	5.7	0.5	7.2	7.1	0.7
154.2	7.0	6.9	0.5	9.3	9.2	0.8
			65 MeV			
31.8	4.3	4.0	0.8	15.7	15.3	1.7
45.6	4.6	4.6	0.7	6.4	6.2	0.7
63.2	1.1	1.0	0.2	2.5	2.4	0.4
81.4	0.7	0.7	0.1	0.8	0.8	0.1
95.7	1.3	1.2	0.3	2.0	1.9	0.4
107.5	3.6	3.5	0.5	4.2	4.0	0.6
120.0	4.8	4.7	0.5	5.9	5.8	0.6
134.5	7.0	6.8	0.8	8.4	8.2	0.9
154.2	8.8	8.6	0.9	10.3	10.1	1.0

TABLE X. Berkeley data.

$\theta_{c.m.}$ (deg)	$d\sigma^+/d\Omega$ (mb/sr)	ϵ_+ (mb/sr)	$d\sigma^-/d\Omega$ (mb/sr)	ϵ_- (mb/sr)	$\theta_{c.m.}$ (deg)	$d\sigma^+/d\Omega$ (mb/sr)	ϵ_+ (mb/sr)	$d\sigma^-/d\Omega$ (mb/sr)	ϵ_- (mb/sr)
		51 MeV					68 MeV		
31.5	1.516	0.140	5.192	0.254	31.6	4.031	0.190	7.299	0.273
36.7	1.611	0.136	3.969	0.166	36.8	3.612	0.176	5.312	0.361
41.9	1.223	0.093	2.978	0.145	42.0	3.247	0.135	4.494	0.164
47.1	1.131	0.093	2.033	0.107	47.2	2.651	0.126	3.082	0.223
62.5	0.434	0.024	0.560	0.025	62.7	0.722	0.025	0.925	0.034
67.6	0.266	0.023	0.371	0.020	67.8	0.437	0.020	0.512	0.026
72.7	0.323	0.020	0.269	0.019	72.9	0.382	0.018	0.366	0.022
77.8	0.375	0.023	0.314	0.020	78.0	0.447	0.019	0.388	0.025
82.8	0.581	0.026	0.427	0.023	83.1	0.692	0.025	0.556	0.030
92.9	0.993	0.050	0.950	0.041	93.1	1.350	0.047	1.180	0.051
102.8	1.610	0.057	1.638	0.053	103.0	2.094	0.063	2.018	0.069
122.5	3.433	0.144	3.715	0.132	122.7	4.011	0.149	4.392	0.142
132.2	4.095	0.164	4.471	0.148	132.4	4.961	0.176	5.098	0.163
141.8	4.764	0.177	4.791	0.147	142.0	5.583	0.213	5.543	0.316
151.4	4.918	0.194	5.034	0.156	151.5	5.843	0.267	5.591	0.333
		60 MeV					75 MeV		
31.5	2.661	0.075	6.712	0.146	31.6	5.940	0.205	9.394	0.236
36.7	2.634	0.071	5.033	0.106	36.9	5.252	0.167	7.080	0.215
41.9	2.327	0.052	3.854	0.076	42.1	4.268	0.141	5.858	0.132
47.1	1.663	0.046	2.835	0.062	47.3	3.006	0.104	3.979	0.127
62.6	0.534	0.010	0.747	0.013	62.8	0.960	0.025	1.119	0.023
67.7	0.366	0.009	0.436	0.009	67.9	0.623	0.019	0.667	0.017
72.8	0.325	0.008	0.306	0.008	73.0	0.458	0.017	0.488	0.014
77.9	0.375	0.008	0.336	0.009	78.1	0.529	0.019	0.498	0.015
83.0	0.618	0.012	0.521	0.011	83.2	0.776	0.023	0.710	0.018
93.0	1.128	0.021	1.077	0.021	93.2	1.413	0.042	1.325	0.035
102.9	1.928	0.031	1.916	0.031	103.1	2.203	0.057	2.361	0.050
122.6	3.936	0.079	4.232	0.083	122.8	4.508	0.143	4.578	0.103
132.3	4.592	0.104	4.875	0.109	132.4	5.264	0.152	5.379	0.116
141.9	5.422	0.150	5.454	0.153	142.0	6.054	0.175	5.646	0.169
151.5	5.721	0.196	5.924	0.203	151.6	6.114	0.200	6.046	0.203

bin, then

$$\bar{\mu}=\int_{\mu_L}^{\mu_U}\mu\frac{d\sigma}{d\Omega}(\mu)d\mu\Big/\int_{\mu_L}^{\mu_U}\frac{d\sigma}{d\Omega}(\mu)d\mu. \tag{B1}$$

Since $(d\sigma/d\Omega)(\mu)$ is not known *a priori*, we use the linear approximation

$$\bar{\mu}\approx\frac{\mu_U(d\sigma/d\Omega)(\mu_U)+\mu_L(d\sigma/d\Omega)(\mu_L)}{(d\sigma/d\Omega)(\mu_U)+(d\sigma/d\Omega)(\mu_L)} \tag{B2}$$

(which, looking at the Berkeley data, should be fairly good in the forward and backward directions, where the problems are), and use the extremes of the $\Delta d\sigma/d\Omega$ bin as $(d\sigma/d\Omega)(\mu_U)$ and $(d\sigma/d\Omega)(\mu_L)$. Finally, to keep the $d\sigma^{(-)}$ and $d\sigma^{(+)}$ data at the same θ, we transform the correction from θ to $d\sigma/d\Omega$ by simple proportions within each data bin. The modified Northwestern data, also shown in Table IX, are still in disagreement with the Berkeley data.